

FINAL REPORT FOR
LIFETIME PREDICTION OF MATERIALS
EXPOSED TO THE NATURAL SPACE
ENVIRONMENT

NASA-39131-DO#8

4/9/1992 to 4/8/1993

Submitted to
NASA
Marshall Space Flight Center, AL 35812

by

Ralph Zee
Principal Investigator
Materials Engineering Program
Auburn University, AL 36849

Tel: (205) 844-3320
Fax: (205) 844-3400
email: rzee@eng.auburn.edu

**LIFETIME PREDICTION OF MATERIALS EXPOSED
TO THE NATURAL SPACE ENVIRONMENT**

NASA-NAS8-39131-DO8, Duration: 4/9/92 - 4/8/93

Final Report Submitted to
NASA
Marshall Space Flight Center, AL 35812

Ralph Zee, Principal Investigator
Materials Engineering Program, Auburn University, AL 36849
Tel: (205) 844-3320, Fax: (205) 844-3400, email: rzee@eng.auburn.edu

Table of Contents

I.	Abstract of the Investigation	1
II.	Introduction	2
III.	Objectives	2
IV.	Results and Discussion	3
	(A) Modeling and Lifetime Prediction	3
	(B) Development of Stress Relaxation Testing Method	34
	(C) Effects of Inert Gas	35
	(D) Effects of Vacuum	41
	(E) Relaxation in Air	42
	(F) Effects of Oxygen	44
	(G) Effects of Gamma Irradiation	48
	(H) Effects of Proton Irradiation	56
V.	Conclusions	64
VI.	References	65

**LIFETIME PREDICTION OF MATERIALS EXPOSED
TO THE NATURAL SPACE ENVIRONMENT**

NASA-NAS8-39131-DO8, Duration: 4/9/92 - 4/8/93

Final Report Submitted to
NASA
Marshall Space Flight Center, AL 35812

Ralph Zee, Principal Investigator
Materials Engineering Program, Auburn University, AL 36849
Tel: (205) 844-3320, Fax: (205) 844-3400, email: rzee@eng.auburn.edu

I. Abstract of the Investigation

The goal of this study is to model the lifetime of different types of seal materials based on results obtained from accelerated experiments. A semi-mechanistic approach was taken. Thermal aging data were taken from the literature whereas experiments were conducted at Auburn under this contract for selected environments. The seal materials of interest are Silicone 383, Silicone 650, Viton 835 and Viton 747. The conditions relevant to this study include thermal, oxygen, inert gas, vacuum and gamma radiation. Compression set data available from NASA were used to examine the thermal effect. Experiments were conducted at Auburn University and at NASA to isolate the role of thermal, oxygen, inert gas, vacuum, gamma irradiation and proton irradiation. A simple discrete stress relaxation method was developed to determine the relaxation response of the elastomers. Dynamic mechanical thermal analysis was also used to characterize the mechanical response of the specimens. These provide a more meaningful correlation between mechanisms and degradation.

II. Introduction

The environment in space is very much different than that on earth. The space environment has been shown to induce degradation in materials under prolonged exposures. Space exposure of materials relevant to space applications has resulted in various forms and degrees of degradation after six years. Elastomeric materials can be particularly sensitive to such exposure due to the bond nature of polymer. In many instances, elastomeric materials are used as sealing materials which separate the manned chamber from the vacuum external environment. In order for the sealing materials to function properly, they must retard a certain degree of residence over their lifetime. To evaluate the materials for long duration missions that extend to thirty years, accelerated testing and lifetime modeling must be used to guide the selection of the appropriate materials for such critical applications.

III. Objectives

The objectives of this investigation are to

1. Develop experimental techniques and modeling approaches for predicting lifetime,
2. Isolate the effects of oxygen, vacuum, inert gas from other thermal components of the degradation process,
3. Determine the role of irradiation of high energy gamma and protons on the behavior of the elastomers.

The materials examined include V835, S650, S383 and to a lesser extent V747. The approach taken was a concerted accelerated testing methodology to predict the long term performance and lifetime of these materials. The temperature range investigated was from ambient to 130°C. A stress relaxation method will be used to evaluate the response of the materials after appropriate exposures.

IV. Research Results and Discussion

Work encompassed in this contract can be divided into modeling and lifetime prediction effort based on existing data and development of semi-mechanistic models; and experimental effort to investigate the effects of temperature, air, oxygen, inert gas and radiation on the degradation of relevant seal materials.

(A) Modeling and Lifetime Prediction

Effort in this area has been concentrated on formulating a simple lifetime prediction scheme based on the compression set data generated by Mr. Morris of NASA. These data were obtained from compression set experiments conducted from ambient to 200°F on both silicone and viton rubber materials. Compression set C_s was defined as

$$C_s = 100(T_o - T_r) / (T_o - T_c) \quad [1]$$

where T_o is the original thickness of the sample, T_r is the final thickness after compression set and recover and T_c is the compression set thickness. Squeeze values from 10 to 40% were used. After examining the data in more detail, we have decided not to convert the data to stress relaxation equivalent. Instead the compression set data were used directly with the basic assumption that the degradation process is completely controlled in a thermal manner. These data are shown in Figures A1 to A11 for the four materials investigated by Morris at different temperatures and squeeze levels as indicated. A master curve was derived for each of the three materials of interest under one specific squeeze condition and these curves are given in Figures A12 to A22. The vertical axis is log of the compression set (not linear) and the horizontal axis is the log of the product of time and $a(T)$ where $a(T)$ is the shift parameter which is related to the activation energy of the thermal degradation process. Here

$$a(T) = A \exp(-E_a/RT) \quad [2]$$

where E_a is the activation energy, A is the pre-exponential constant, R is the gas constant and T is the absolute temperature. Each of these curves represent data from five temperatures from ambient to 200°F. The rate of compression relaxation is a strong function of temperature. If the data were plotted without the $a(T)$ parameter, the lines from different temperatures would be offset from one another with the

highest temperature at the left side. The parameter $a(T)$ increases exponentially with temperature. With the convention that $a(T)=1$ at room temperature, that is the room temperature line does not move, the value $a(T)$ for each temperature can be calculated by determining the amount of shift needed for each temperature so that all the data lie on the same line. This shift process was applied to the data of Morris. Each of the three materials was squeezed to different levels at different temperatures. It was decided that within each material, the parameter $a(T)$ must be the same at each selected temperature for all levels of squeeze. The condition ensures the self consistency of the analysis. As evident from the master curves presented in Figures A12 to A22, the results are quite satisfactory. In addition within each material, the master curves for different squeeze levels overlap one another indicating the independence of the thermal process which is consistent with the assumption that the only influential parameter in the deformation process is temperature. The temperature dependence of $a(T)$ yields the activation energy for the thermal process. These energies were found to be 12, 18, 9 and 8.5 kcal/mole for V835, S650, S383 and V747 respectively. The values of A for the materials are 6.83×10^8 , 1.78×10^{13} , 4.22×10^6 and 1.81×10^6 . These constants are necessary for normalization purpose so that the value of $a(T)$ equals unity at room temperature. These values are within the range obtained for other elastomer systems.

The master curves can be used to predict lifetime in the following manner. Let us assume that one is concerned with S650 and that the maximum compression set one

allows is 10%. One then first locates 10^1 on the y-axis on either Figure A15, A16 or A17. Notice that the three curves are almost identical. The x-axis value for 10% set is approximately 120 days. This corresponds to the value of $a(T)*t$ that would result in failure of the seal. At room temperature, $a(T)$ is one implying a lifetime of 120 days. At an elevated temperature of 160°F, $a(T)$ is 65.7 resulting in a lifetime of approximately 2 days.

A detailed literature search was conducted to examine other models appropriate for the thermal physical degradation of elastomers. For most polymers, the original shape of the specimens may be partially or fully recovered after the thermomechanical load is released. Incomplete recovery may be caused by viscous flow, time-dependent (retarded) deformation, or structural changes at the molecular level. Plastic deformation and failure processes of glassy or crystalline polymers are not considered in the present report. Potential alterations of molecular structures (e.g. chain scission or cross-linking induced by heat and/or UV) may also give rise to a stress relaxation or decay behavior. This is referred to as "chemical stress decay" or "chemical stress relaxation".

On the molecular level the present model considers the relaxation process to be related to the transition between two conformational states of a molecular chain segment and/or slippage between neighboring chain segments. This is a modified version of the Site Model Theory [6], which is based on the transition state theory [3]. In its simplest form there are two chain conformational states, separated by an energy

barrier of U_0 . For further simplicity we may assume that, in the absence of an external stress field, the probability that the chain segment is in State 1 is equal to that in state 2:

$$N_1^0 = N_2^0 = N/2 \quad [3]$$

$$N_1 + N_2 = N_1^0 + N_2^0 = N \quad [4]$$

where N_1 = the occupation number of state 1 ($N_1 = N_1^0$ at time zero prior to the application of the stress), N_2 = the occupation number of state 2, and N = the total number of states per unit volume. The "state" here may also refer to the state before and the state after chain slippage occurs.

To give rise to a relaxation process, the energy barrier (activation energy) must be altered by the application of the imposed stress field in such a fashion that it lowers the effective energy barrier in the forward transition while it raises the required energy barrier for a backward change. This would then induce a change in the population of state 1 and state 2 and such conformational state transitions relate directly to strain or, in the present context, compression set. One may perhaps imagine that this could arise if, for instance, the uncoiling of a chain segment involves internal rotations. The chain could possibly be changed from a more crumpled gauche conformational state to a more extended trans state. The stressed chains become mechanically excited and deexcitation can occur by entropy relaxation (conformational

change), enthalpy relaxation (chain slippage, e.q.), or chain scission. A significant part of the strain energy becomes internally dissipated, leading to incomplete recovery such as compression set. It is of interest to note that compression set of seal materials were measured at temperatures ranging from 75°F to 200°F (23°C - 93°C) [1], which are considerably higher than the T_g 's of materials such as silicon rubbers. With a relatively high test temperature and a large time scale, these elastomers fall into the regimes of "rubbery plateau" and "viscous flow" in the dynamic mechanical spectra. The relative importance of these regimes depends largely on the degree of cross-linking (network polymers), physical entanglements (amorphous non-cross-linked polymers), and crystallinity (semi-crystalline polymers). In a non- or lightly cross-linked polymer, long-range segment movements may be activated, leading to significant viscous flow. Viscous flow becomes more difficult to take place when molecular chains are tied together by chemical or physical cross-links.

The transition probability for a jump from state 1 to state 2 in the absence of an external field can be obtained, with the aid of classical statistical thermodynamics:

$$\Gamma^0 = \nu_0 \exp(-U_0/KT) \quad [5]$$

As a consequence of an applied stress σ_0 the probability for the forward jump Γ_{12} and that for the backward jump Γ_{21} will be, respectively,

$$\Gamma_{12} = \nu_0 \exp [-(U_0 - \Delta U)/KT] \quad [6]$$

and

$$\Gamma_{21} = \nu_0 \exp [-(U_0 + \Delta U)/KT] \quad [7]$$

where ΔU is assumed to be given by $\Delta U \approx s\sigma\lambda$. Here, λ is a structural parameter commonly referred to as "activation volume" and s is a stress concentration factor governed by the local structural environment.

Expanding Equations (6) and (7) and making a linear approximation leads to

$$\Gamma_{12} \approx \Gamma^0 (1 + \Delta U/KT) \quad [8]$$

$$\Gamma_{21} \approx \Gamma^0 (1 - \Delta U/KT) \quad [9]$$

The rate equations for state 1 and state 2 are then

$$dN_1/dt = -N_1\Gamma_{12} + N_2\Gamma_{21} \quad [10]$$

$$dN_2/dt = -N_2\Gamma_{21} + N_1\Gamma_{12} \quad [11]$$

which, upon combination, lead to

$$d[(N_2 - N_1)/(N_1 + N_2)]/dt + 2\Gamma^0[(N_2 - N_1)/(N_1 + N_2)] = 2\Gamma^0(\Delta U/KT) \quad [12]$$

This equation is formally identical to the equation of a Kelvin-Voigt Model, with a characteristic retardation time given by

$$\tau = 1/(2\Gamma^0) = 1/(2\nu_0)\exp(U_0/KT) \quad [13]$$

and with $(N_2 - N_1)/(N_1 + N_2) = (N_2 - N_1)/N$ related to the strain, $\epsilon(t)$. It may be noted that the compression set test was performed under a constant deflection (stress relaxation) condition. However, the irrecoverable portion of the strain is essentially a "creep" as the result of an imposed stress (which may be decaying). Our assumption is, therefore that the compression set ($e_{cs} = \epsilon(t)/\epsilon_0$) is directly related to $(N_2 - N_1)/(N\epsilon_0)$:

$$de_{cs}/dt + 2\Gamma^0 e_{cs} = 2\Gamma^0 (\Delta U/KT)/\epsilon_0 \text{ with } \Delta U \approx s\sigma\lambda \quad [14]$$

Now, assume tentatively that the initially applied stress, $\sigma_0 = \epsilon_0 E_u$ does not decay during the compression set test (not a valid assumption). Then, the solution to this differential equation for the case of a constant stress σ_0 applied at $t=0$ is given by

$$e_{cs} = (\Delta U/\epsilon_0 KT)(1 - e^{-t/\tau}) \quad [15]$$

Here, E_u is the stress relaxation modulus of an un-relaxed rubber and $\Delta U \approx s\sigma_0\lambda$. To

reach a specific critical compression set ($e_{cs} = e_c$) would need an elapsed duration of time given by:

$$t_{life} = \ln[1 - e_c KT \epsilon_o / \Delta U]^{-1} [1 / (2\nu_o)] \exp(U_o / KT) \quad [16]$$

The present theory is expected to work better for a real creep test. In the compression set test the stress is in actuality allowed to decay, rather than being kept constant. To obtain a more accurate prediction of the compression set, equation (14) must be solved with $\Delta U \approx s\sigma(t)\lambda$ now being a function of time. This may be accomplished by assuming a stress decay function (e.g., from a Maxwell model) or by embarking on the Boltzmann superposition approach through the use of a standard linear solid model.

V835 10% Squeeze

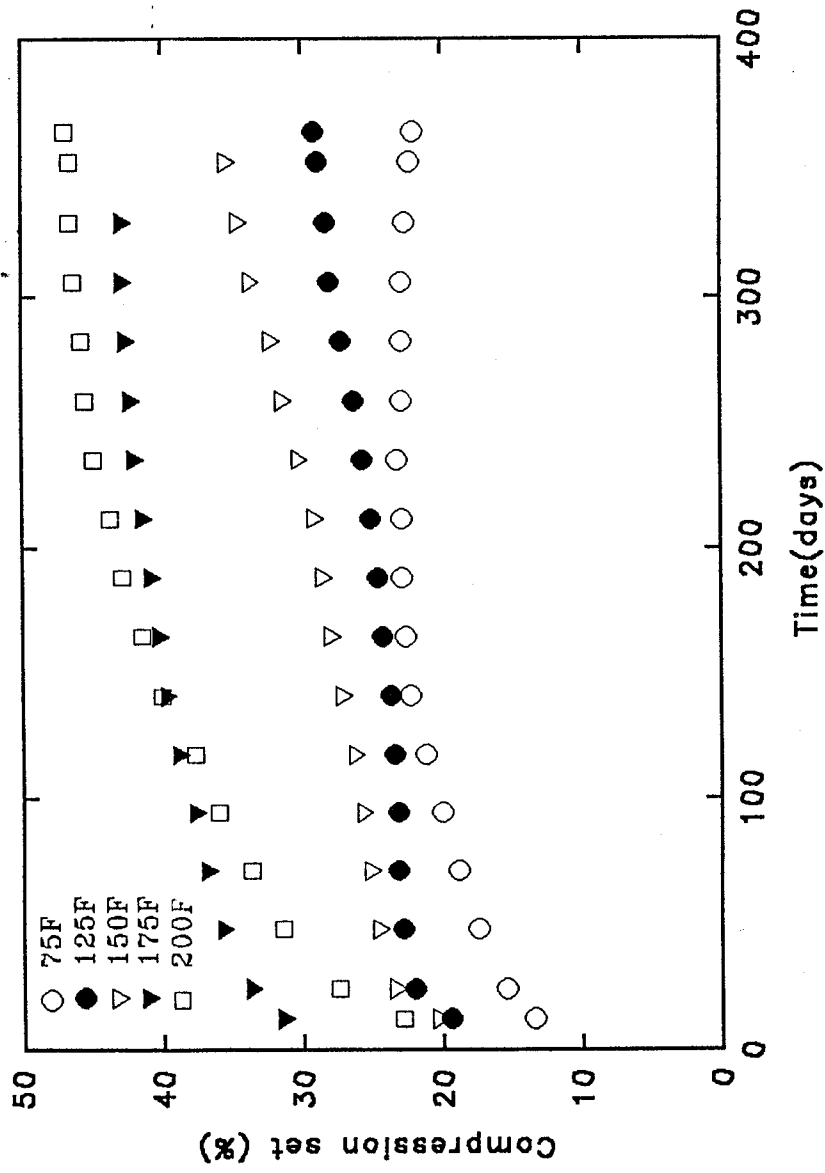


Figure A1. Compression set data for V835 with a 10% squeeze.

V835 20% Squeeze

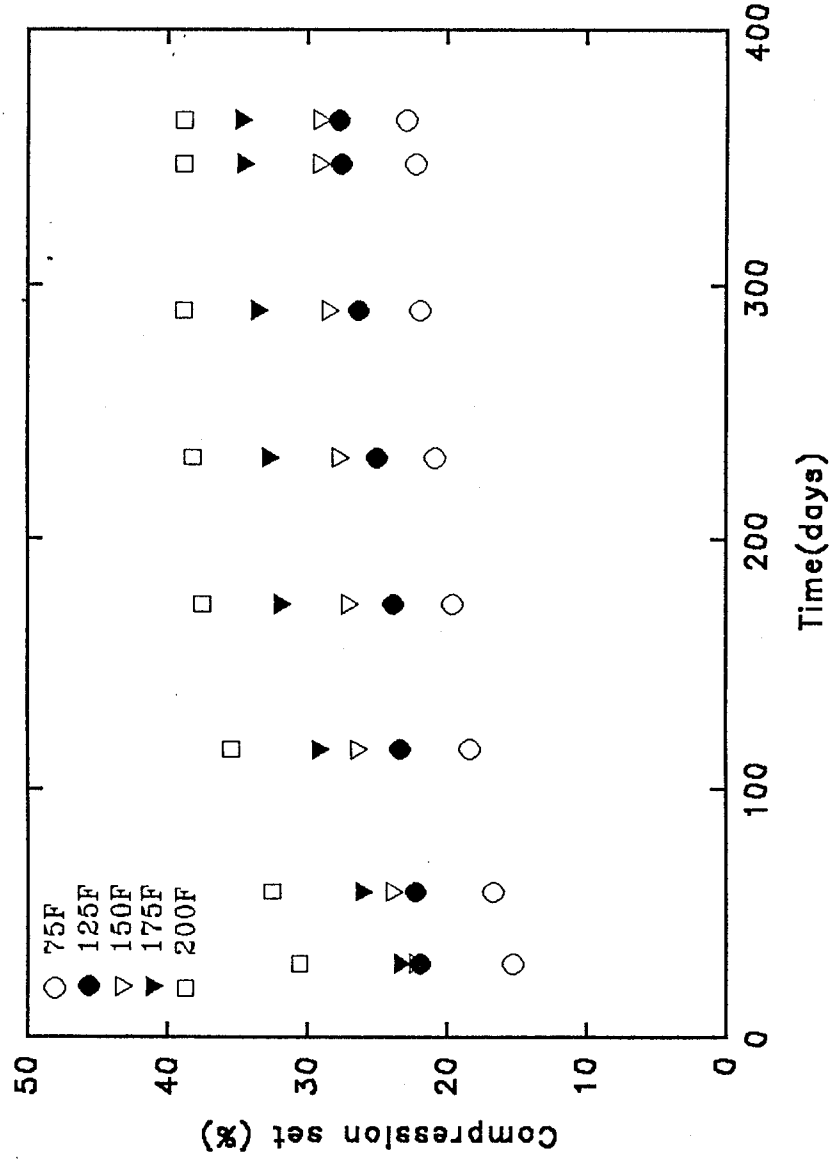


Figure A2. Compression set data for V835 with a 20% squeeze.

V835 40% Squeeze

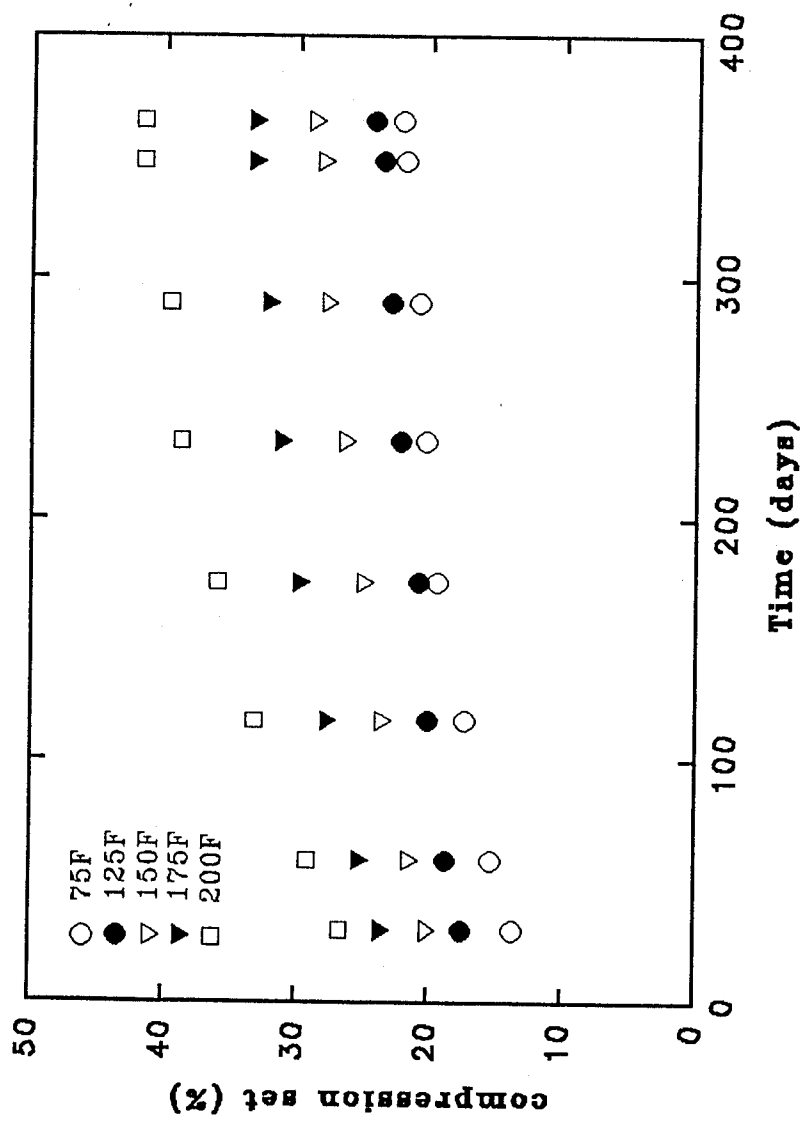


Figure A3. Compression set data for V835 with a 40% squeeze.

S650 10% Squeeze

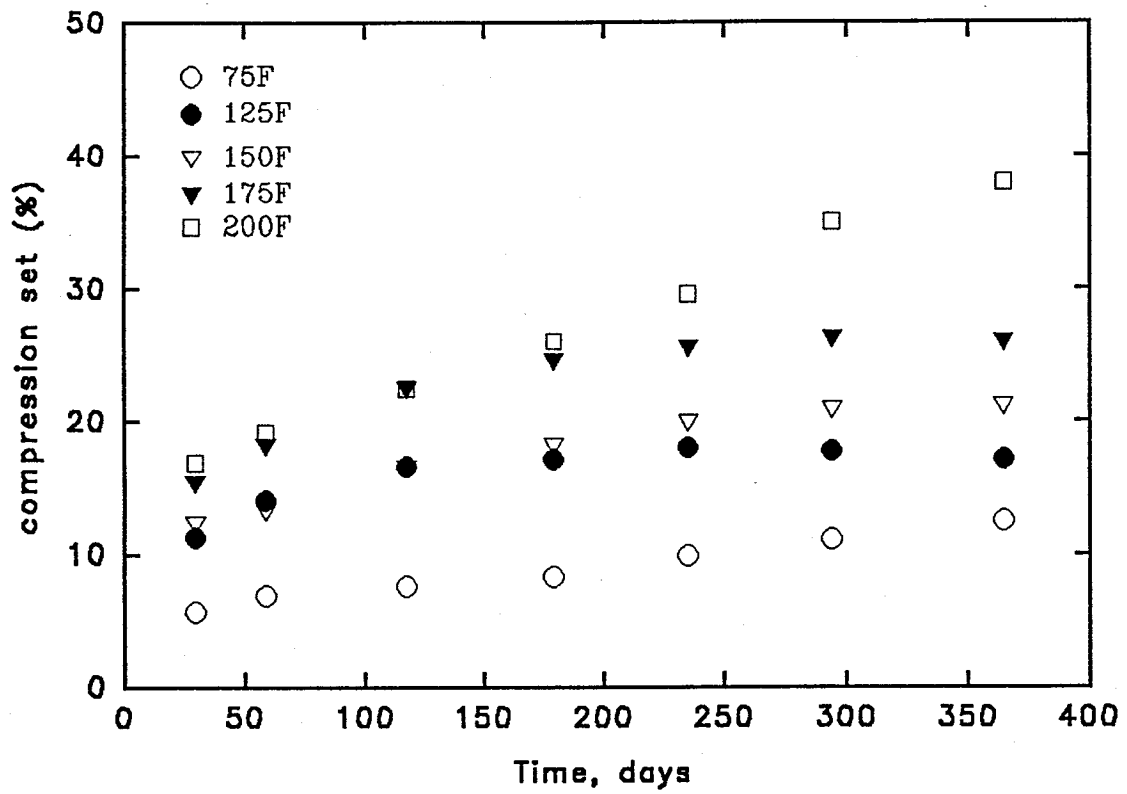


Figure A4. Compression set data for S650 with a 10% squeeze.

S650 20% Squeeze

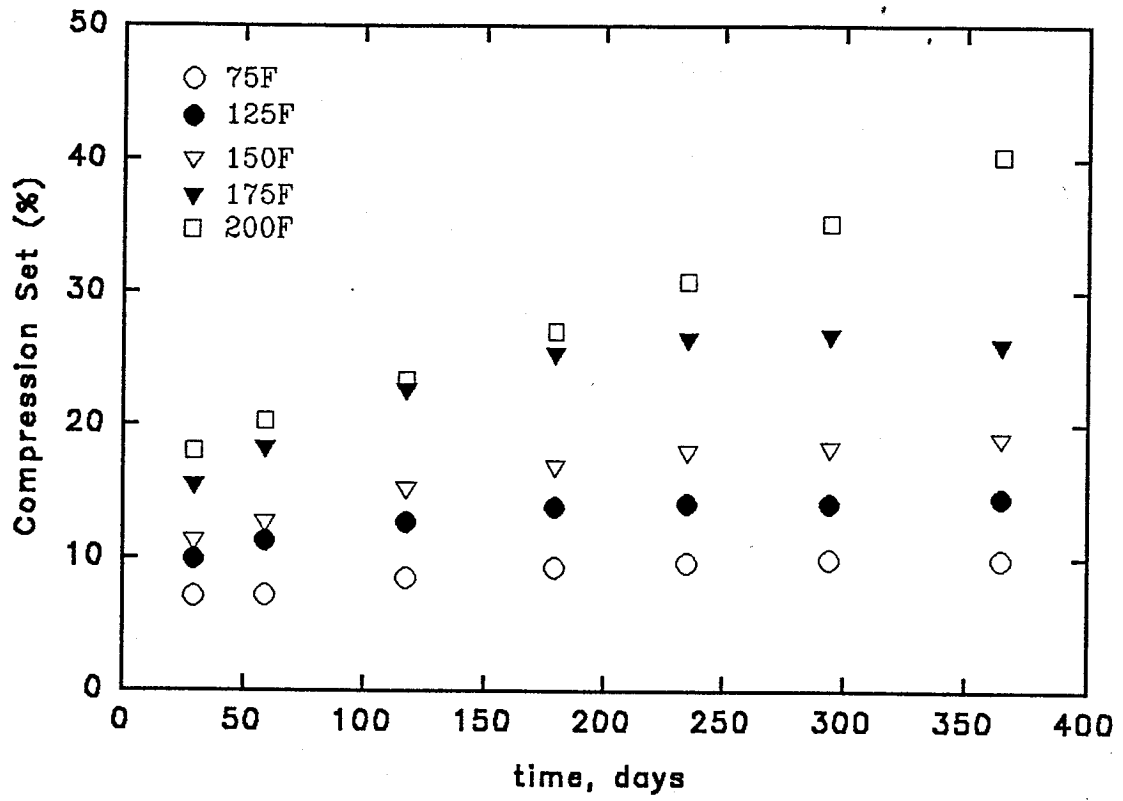


Figure A5. Compression set data for S650 with a 20% squeeze.

S650 40% Squeeze

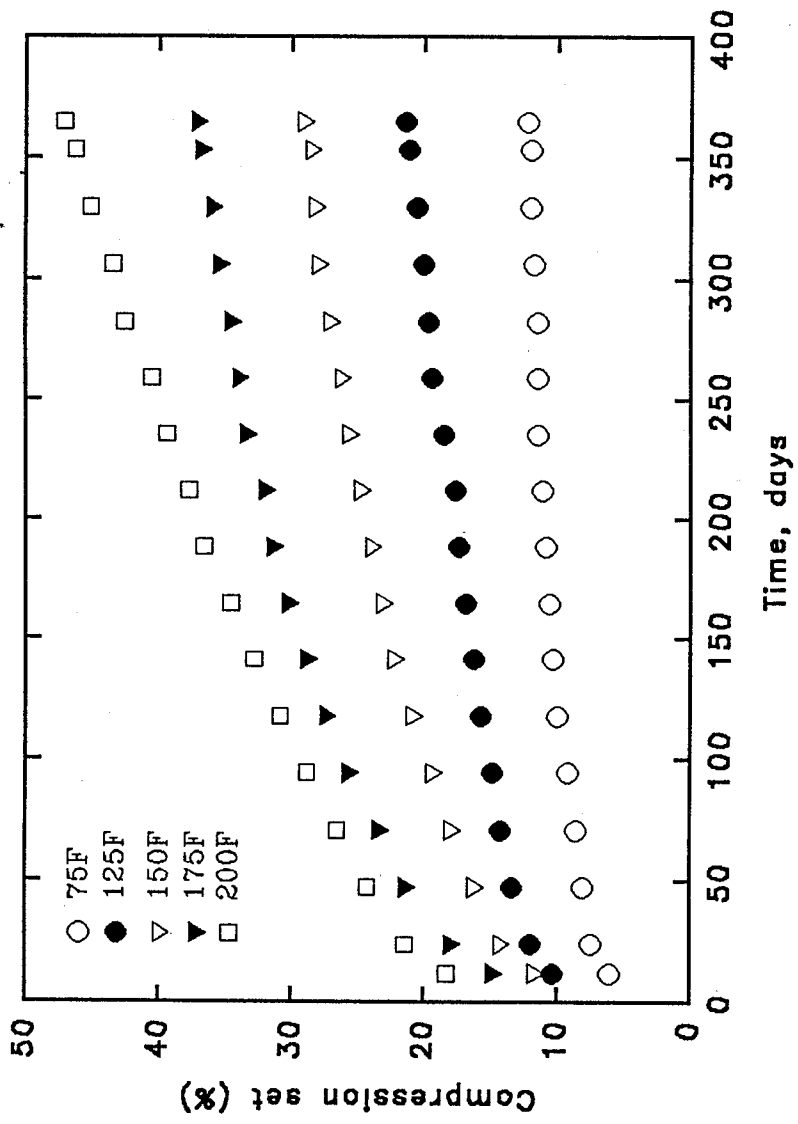


Figure A6. Compression set data for S650 with a 40% squeeze.

S383 20% Squeeze

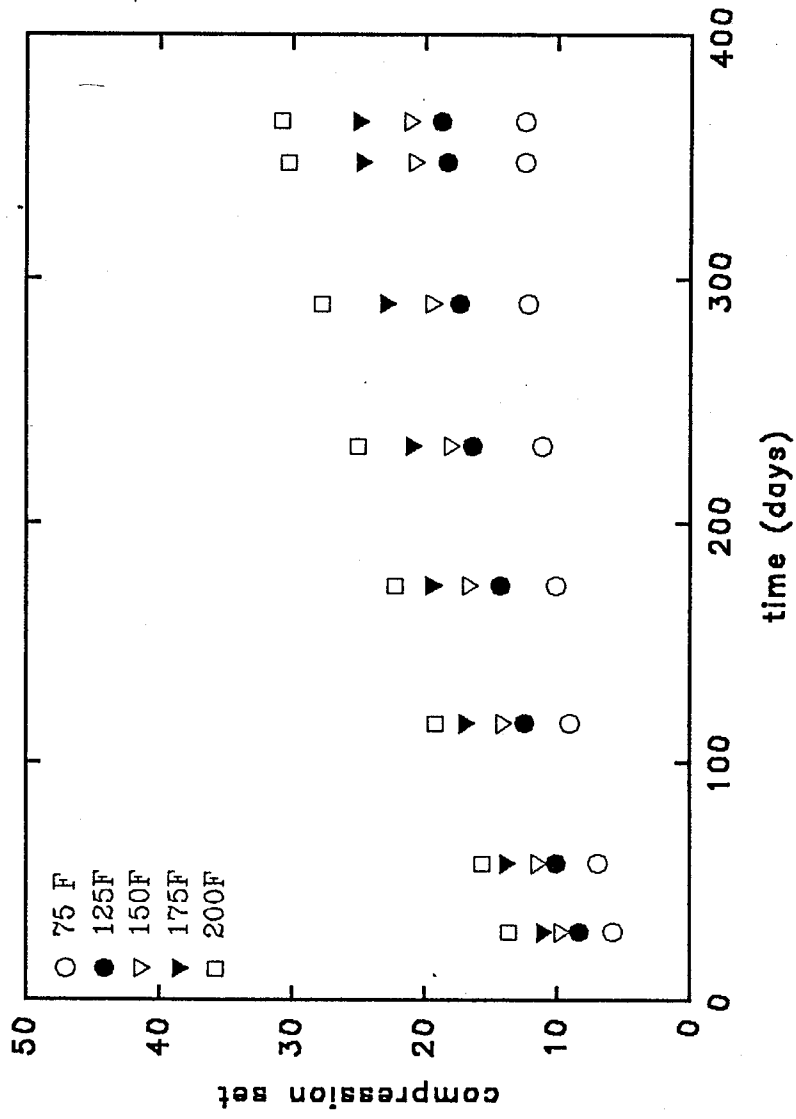


Figure A7. Compression set data for S383 with a 20% squeeze.

S383 40% Squeeze

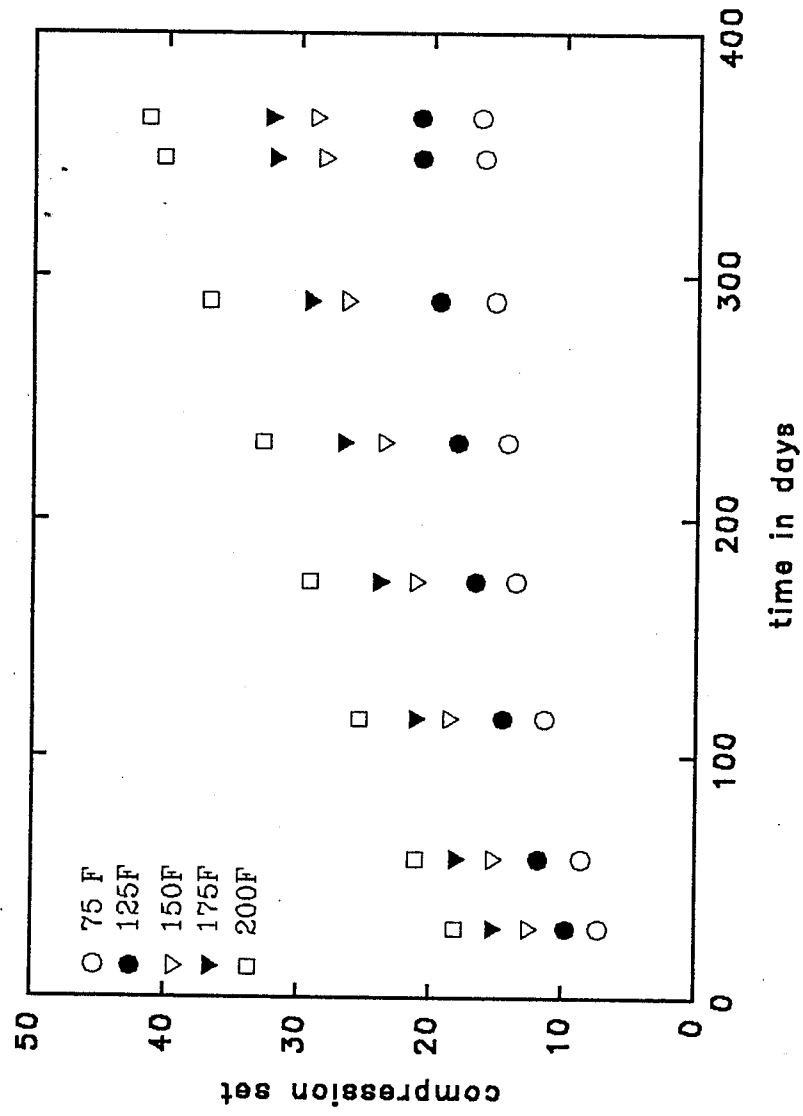


Figure A8. Compression set data for S383 with a 40% squeeze.

V747 10% Squeeze

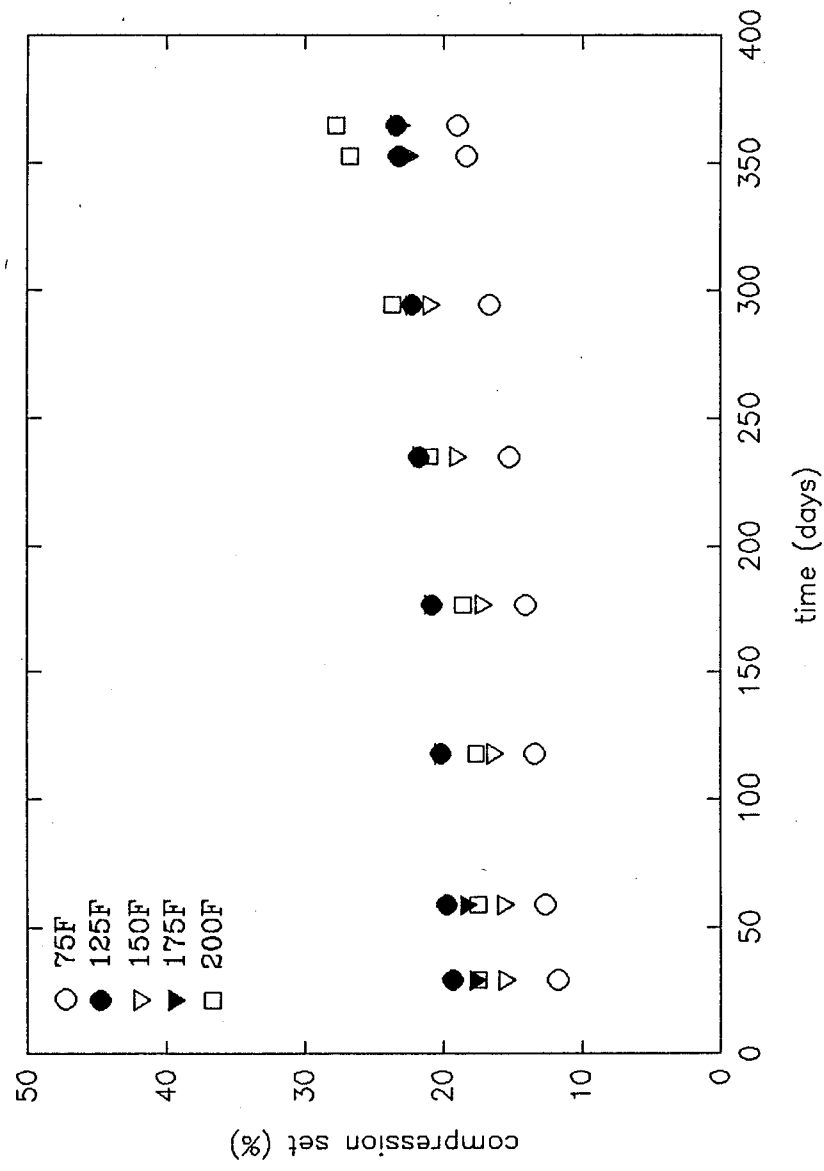


Figure A9. Compression set data for V747 with a 10% squeeze.

V747 20% Squeeze

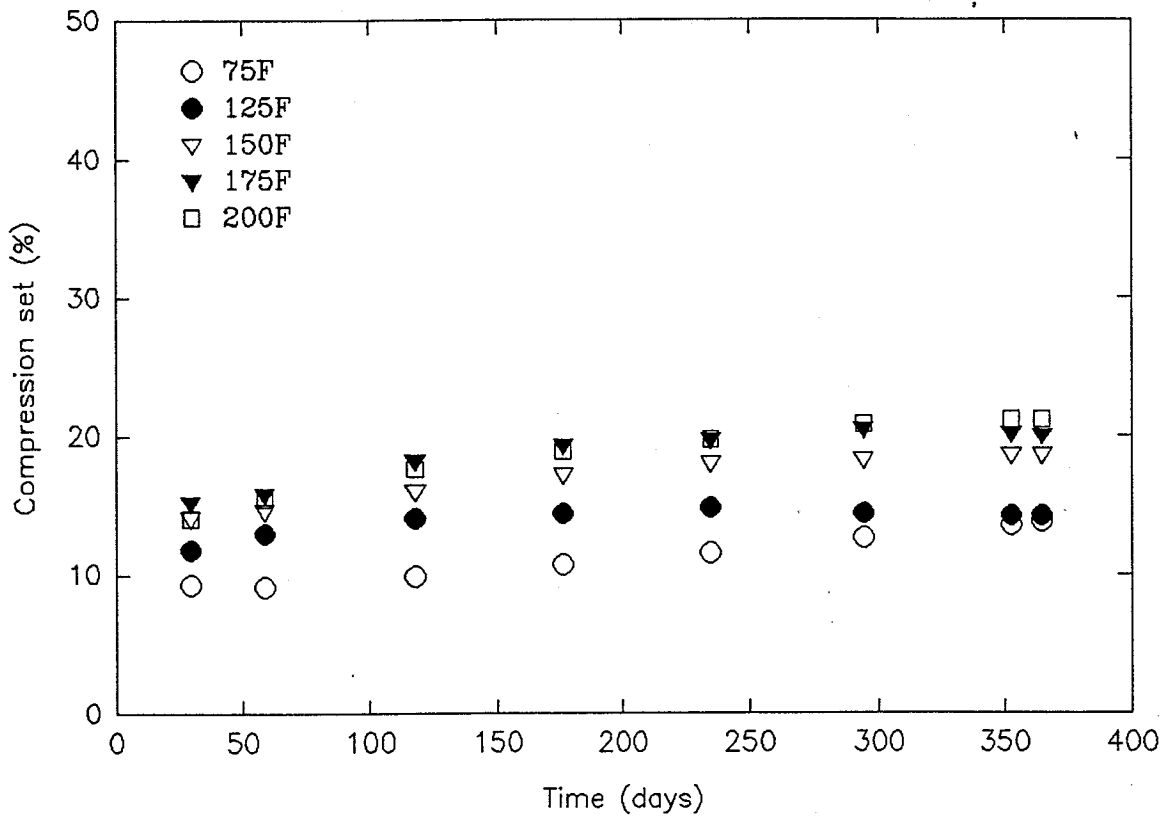


Figure A10. Compression set data for V747 with a 20% squeeze.

V747 40% Squeeze

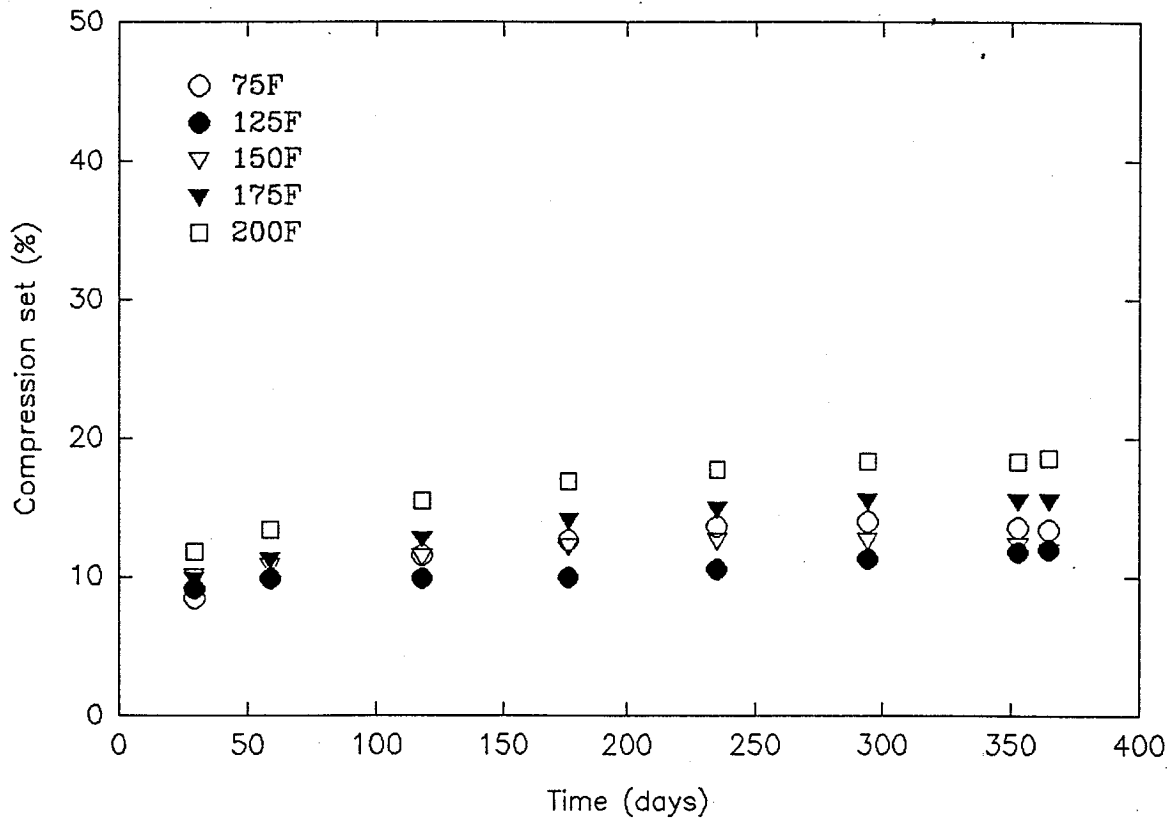


Figure A11. Compression set data for V747 with a 40% squeeze.

V835 10% Squeeze

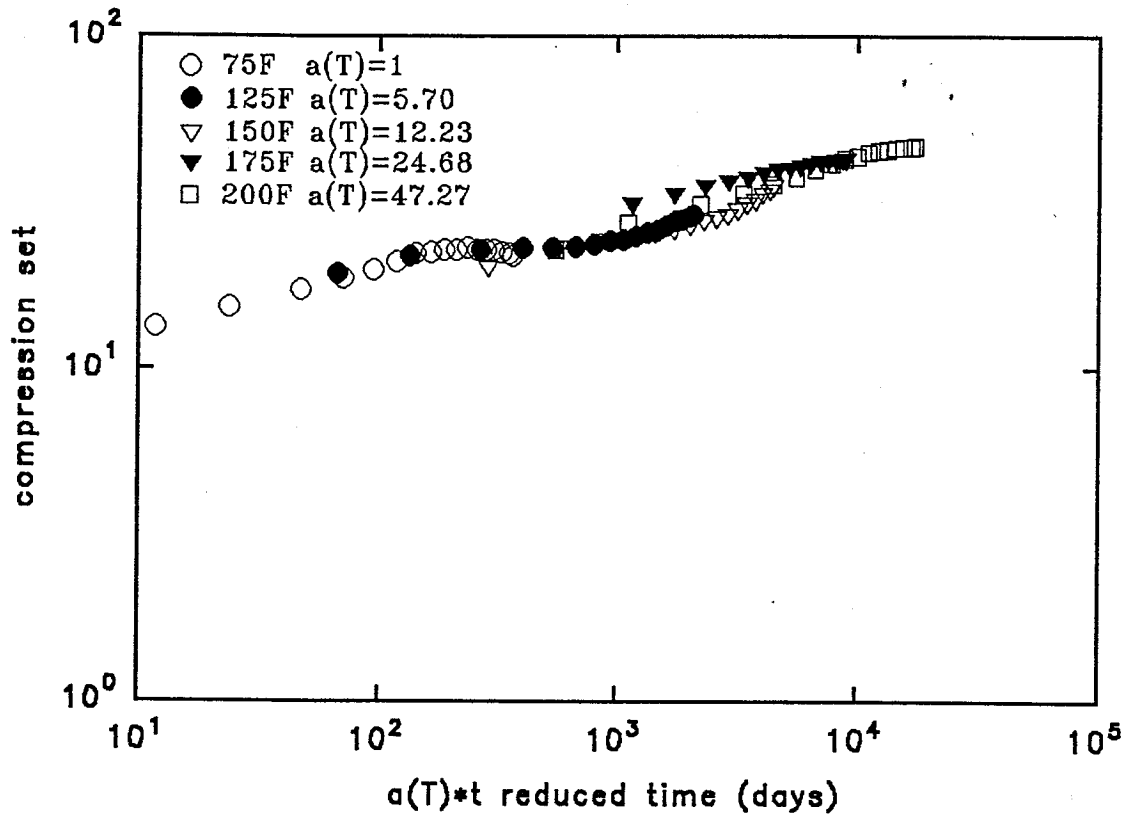


Figure A12. Master curve for V835 with a 10% squeeze.

V835 20% Squeeze

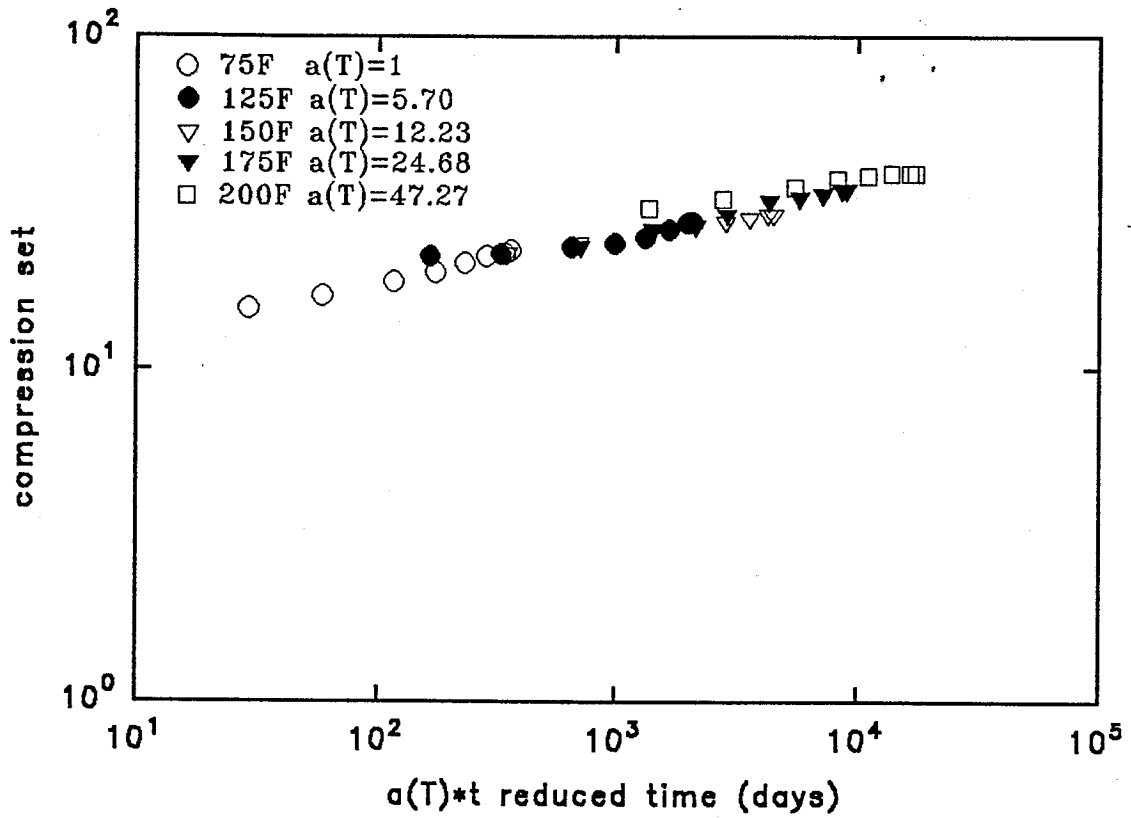


Figure A13. Master curve for V835 with a 20% squeeze.

V835 40% Squeeze

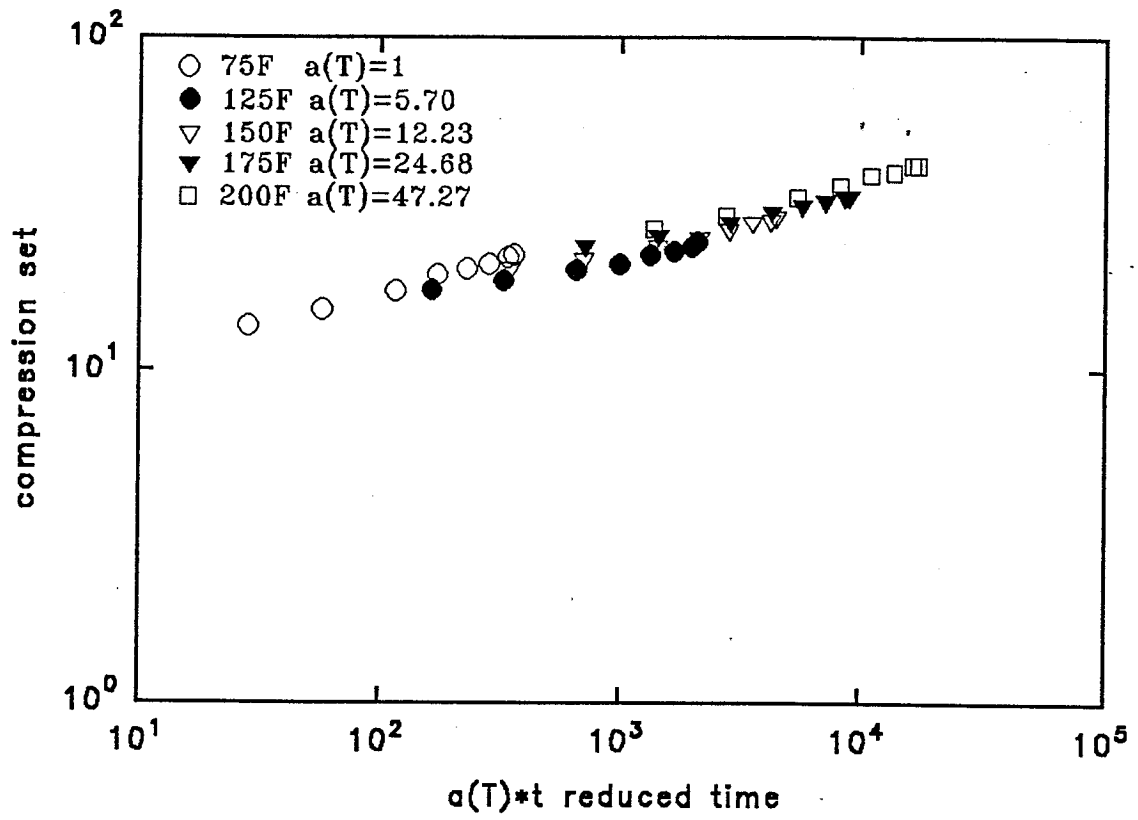


Figure A14. Master curve for V835 with a 40% squeeze.

S650 10% Squeeze

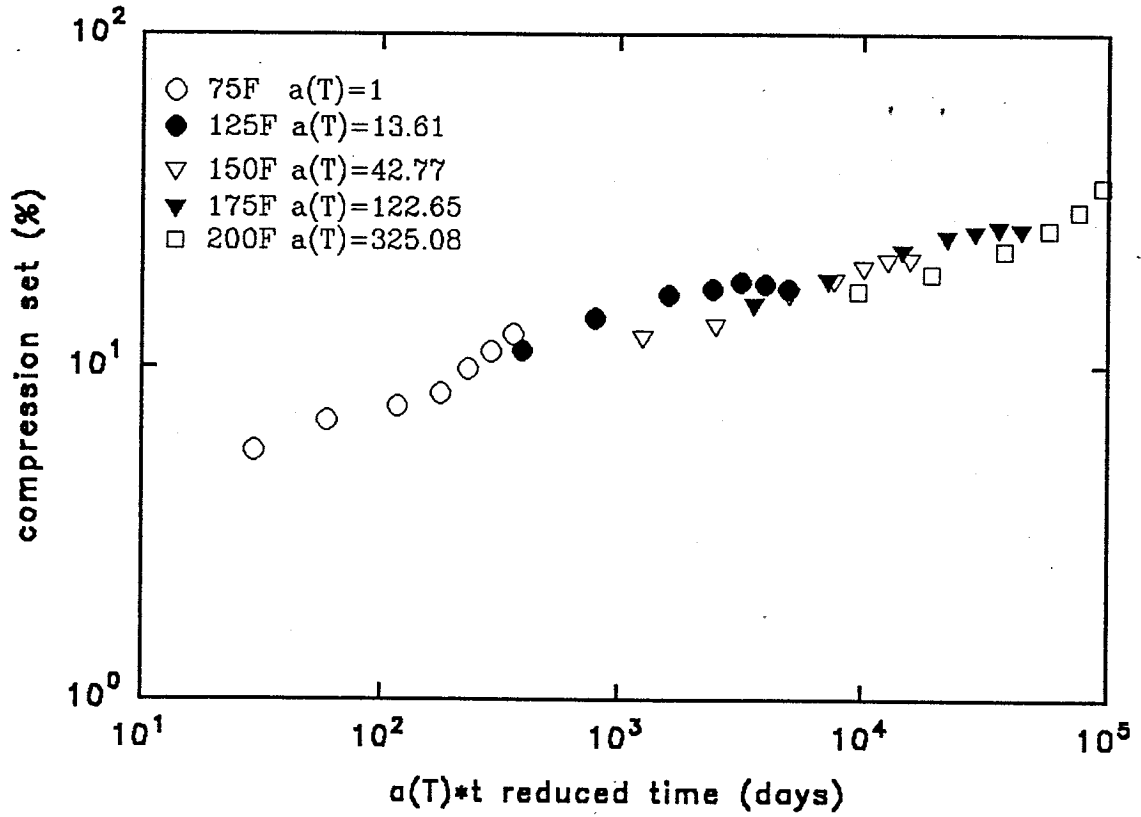


Figure A15. Master curve for S650 with a 10% squeeze.

S650 20% Squeeze

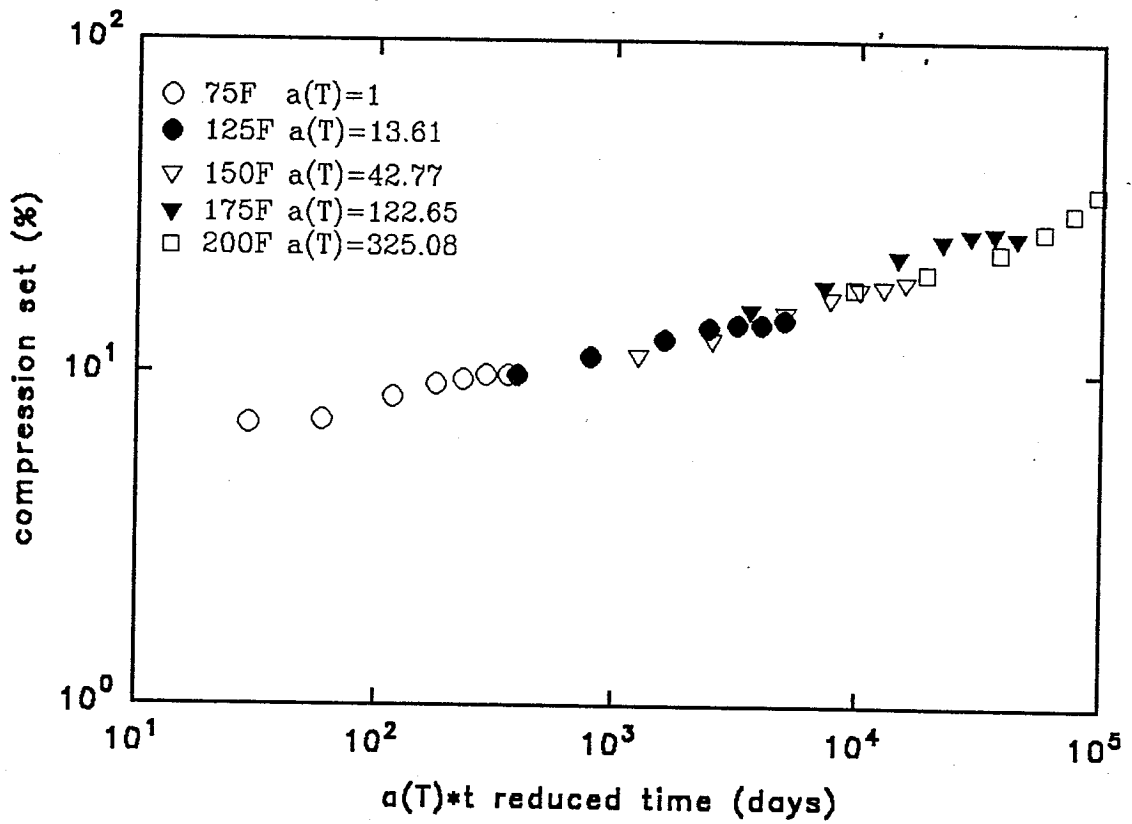


Figure A16. Master curve for S650 with a 20% squeeze.

S650 40% Squeeze

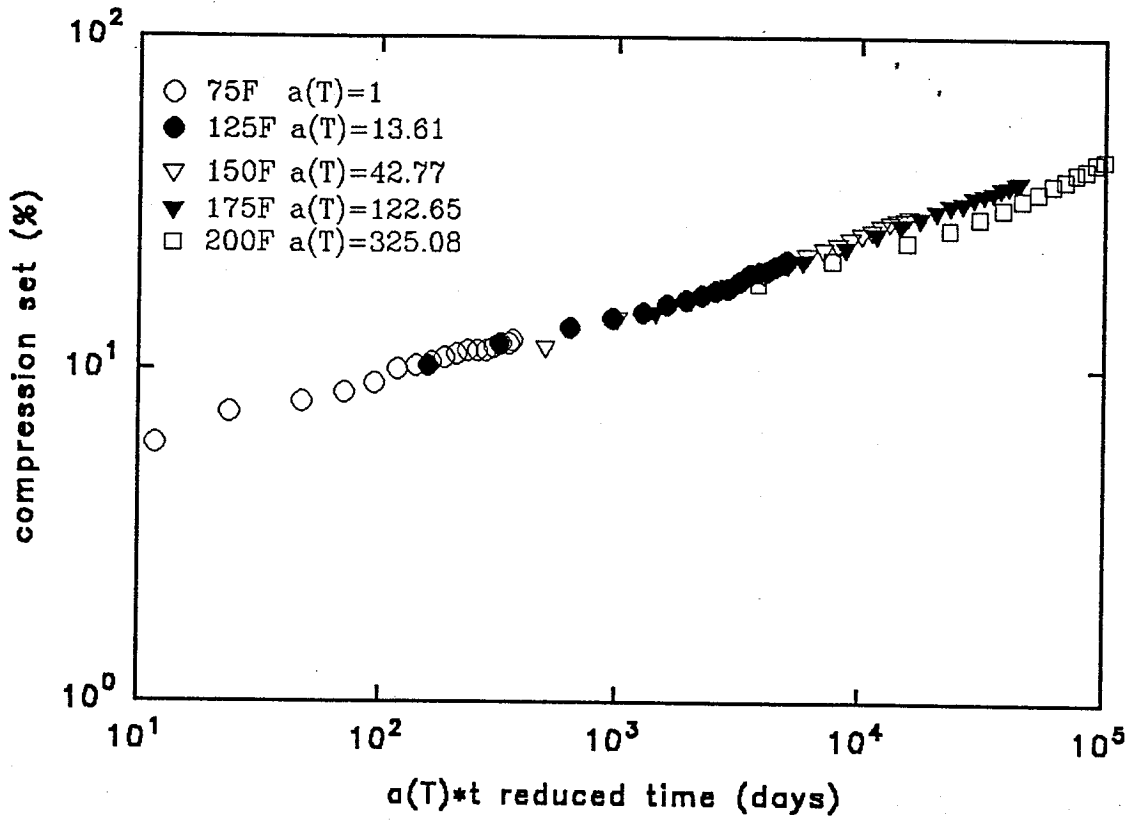


Figure A17. Master curve for S650 with a 40% squeeze.

S383 20% Squeeze

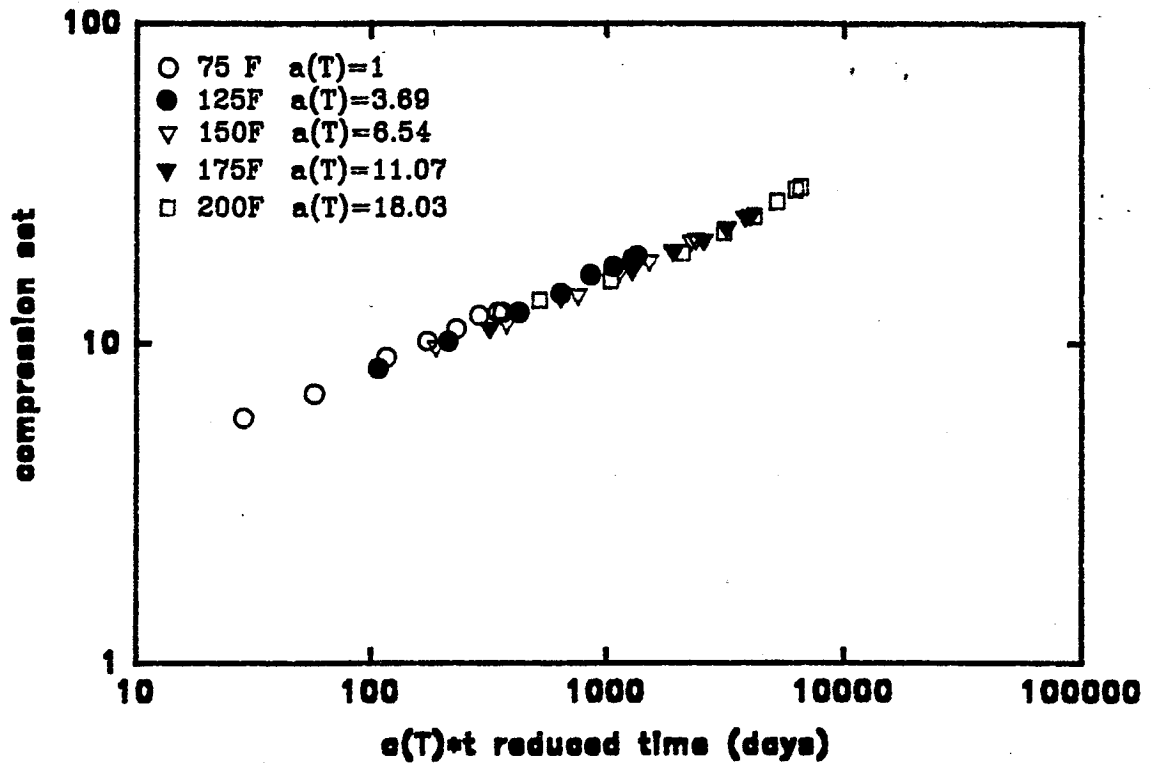


Figure A18. Master curve for S383 with a 20% squeeze.

S383 40% Squeeze

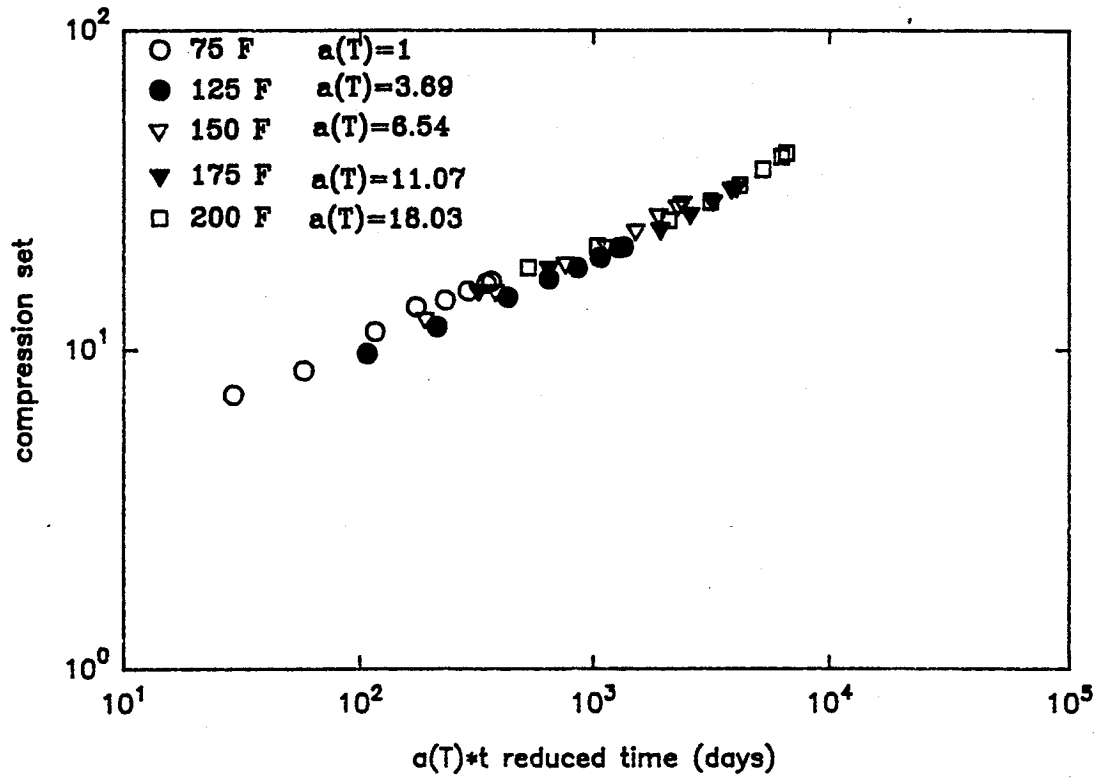


Figure A19. Master curve for S383 with a 40% squeeze.

V747 10% Squeeze

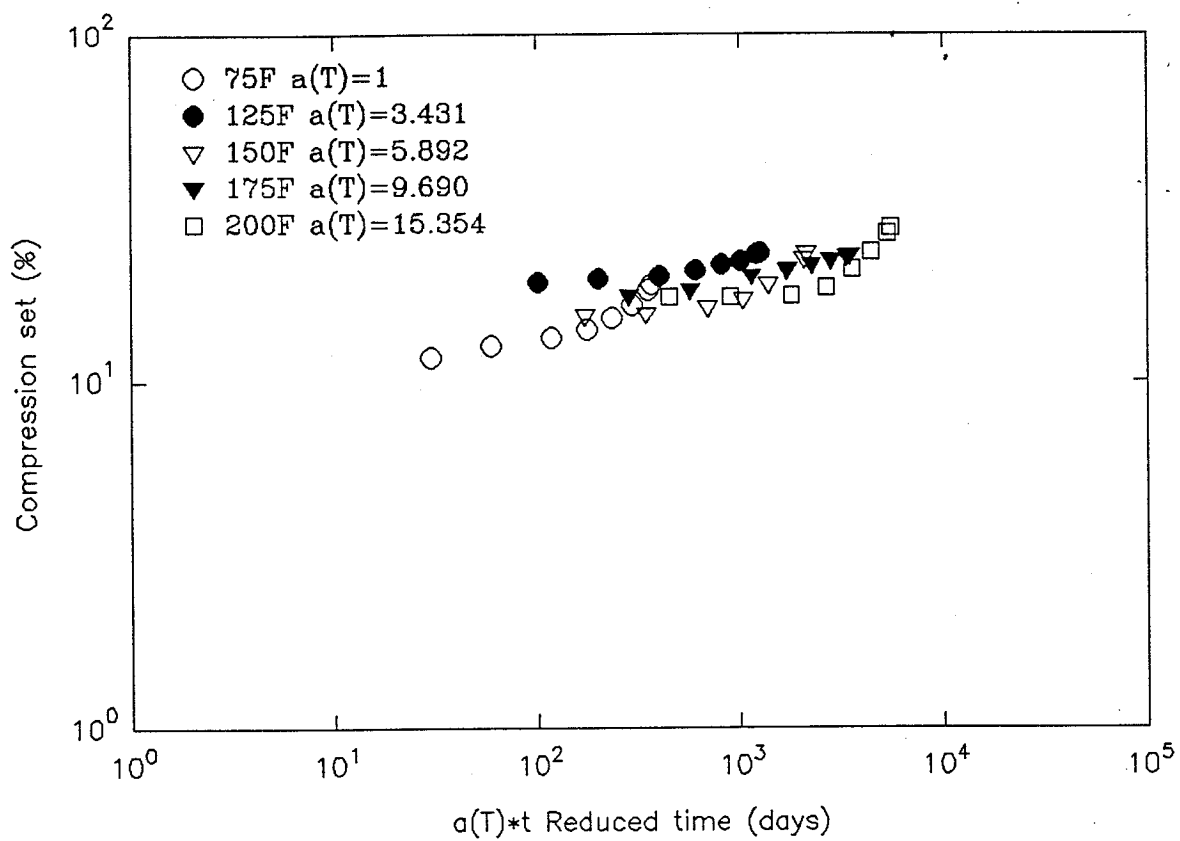


Figure A20. Master curve for V747 with a 10% squeeze.

V747 20% Squeeze

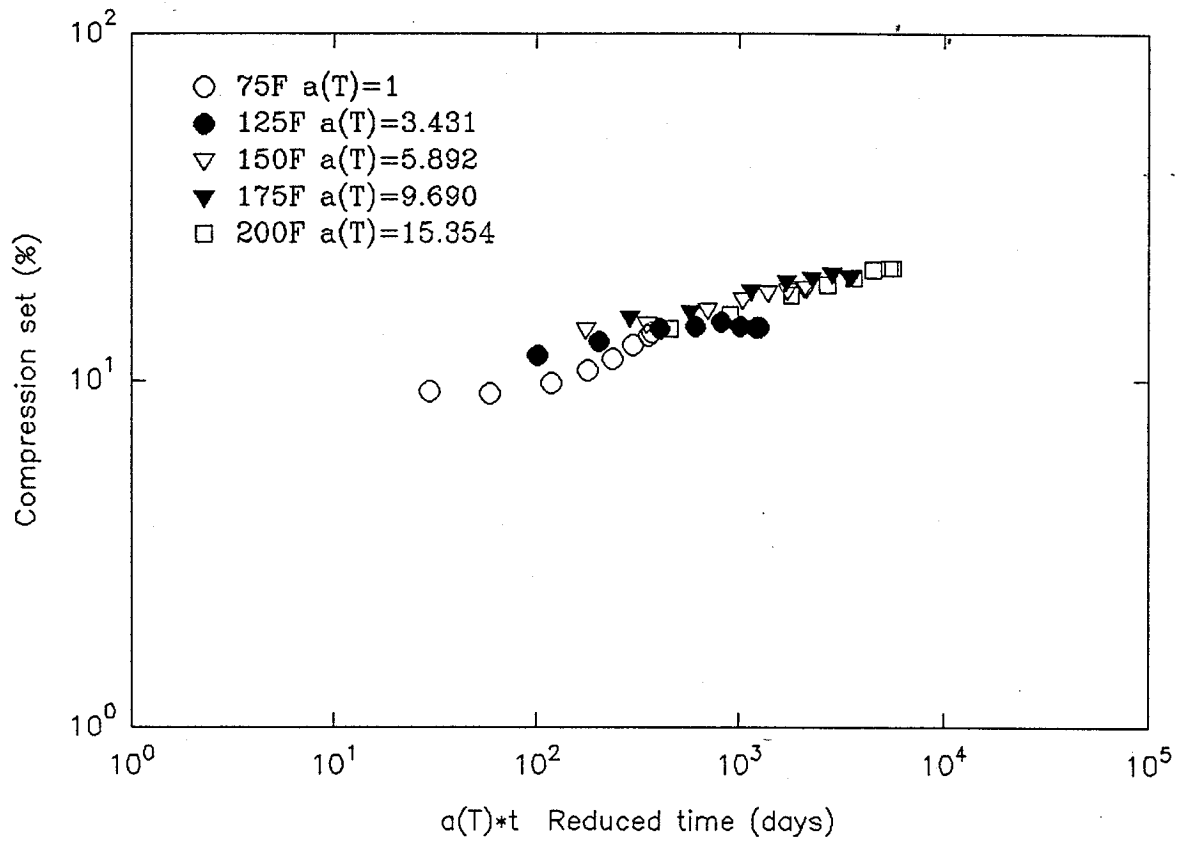


Figure A21. Master curve for V747 with a 20% squeeze.

V747 40% Squeeze

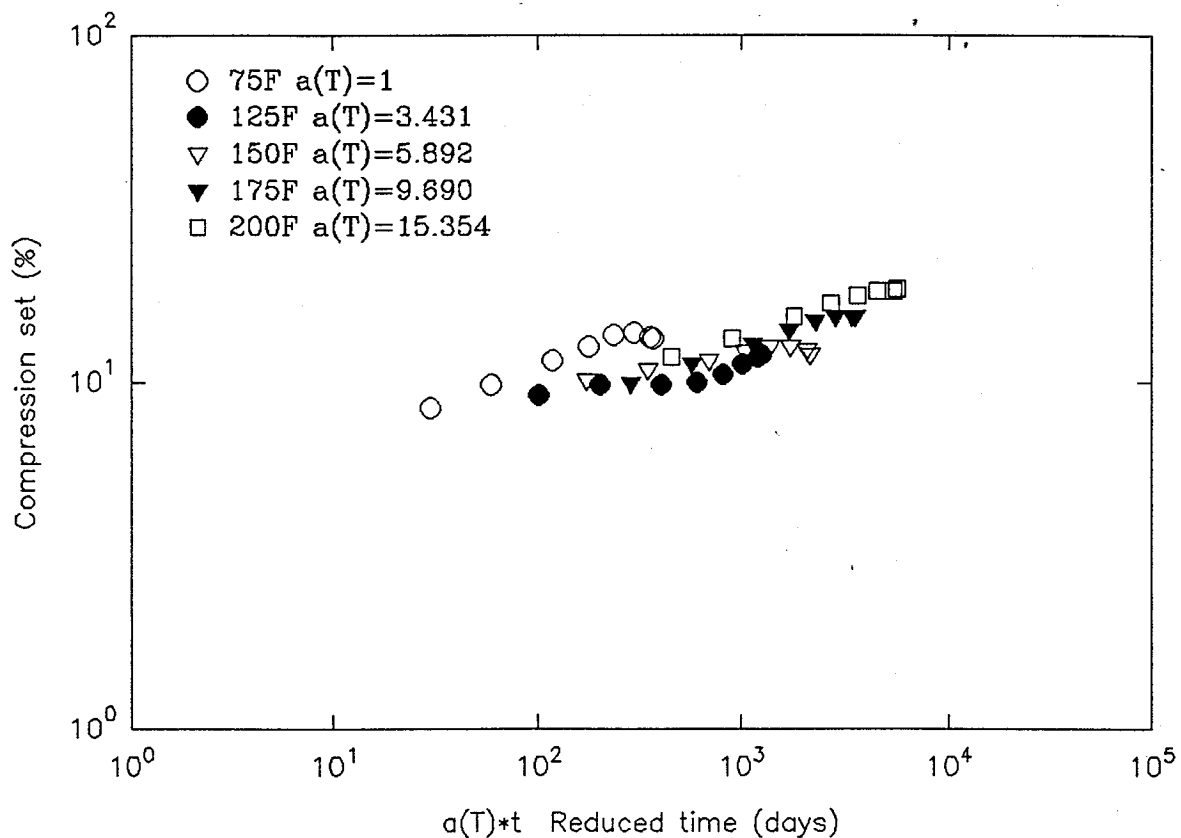


Figure A22. Master curve for V747 with a 40% squeeze.

(B) Development of Stress Relaxation Testing Method

In order to obtain test results more relevant for lifetime prediction, it was decided to develop a test method based on stress relaxation. However, due to the time and fiscal constraints of the project, it was not feasible to conduct detailed stress relaxation tests which would require the dedicated use of a mechanical testing unit and the development of complicated hardware to incorporate the selected environment to the testing unit. In addition, it would permit simultaneous testings. Therefore a discrete stress relaxation method was developed. The elastomeric samples were cut into rectangular strips. The thickness of the samples was 0.125" with a gage width of 0.25". The gage length used was 2". The samples were clamped onto an aluminum holder and were stretched to an engineering strain of 50% (stretched length was 3"). These samples were then exposed to the selected environments for predetermined durations. The samples were relaxed after exposure and the relaxed length was measured immediately followed by periodic measurements up to 24 hours. This was necessary to determine if there were any anelastic effect in the samples. It was found that all the relaxation occurred immediately upon relaxation of the stress. Markers were precisely placed on the surface of the samples prior to stress loading. These markers were 0.5" apart. The distances between these markers were carefully measured and their values averaged after exposure and relaxation. Assuming that the relaxation process is entirely elastic in nature, the time dependent stress in a stress relaxation test can be expressed as

$$\sigma(t) = \sigma_0 \exp(-Kt) \quad [17]$$

where $\sigma(t)$ is the stress required to maintain the strain at time t , σ_0 is the initial stress and K is the relaxation constant (with a unit of inverse t). Since the tests conducted is a measurement of the relaxed length rather than direct stress relaxation and that an initial strain of 50% (or 0.5), equation [17] can be replaced by

$$\epsilon(t) = 0.5 [1 - \exp(-Kt)] \quad [18]$$

where $\epsilon(t)$ is the residual strain measured at time t . Due to the relatively large test matrix encompassed in this study, only a limited number of tests were conducted under each selected environment.

(C) Effects of Inert Gas

Results from the inert gas tests will form the basis for comparison although the actual environment resembles more like vacuum. It was decided to use inert gas as the standard instead of air due to the presence of oxygen in the latter which had a significant influence on the degradation process.

Three experiments were conducted at room temperature, 100°C and 130°C for a fixed duration of one week. Results from this series of tests are provided in Tables C1 to C3. The V835 sample broke prematurely at 100°C and the S383 sample broke

at 130°C. The four columns in the tables under 2", 1.5", 1" and 0.5" correspond to the independent measurements made between the half inch markers placed on the surface of the specimens. The entries under them are the residual strain values. These values were averaged and equation [18] was used to calculate the relaxation constant K (in unit of s⁻¹).

The important observation in this group of materials is that the relaxation rates (a direct measurement of the deformation rate) are very low, all on the order of 10⁻⁸/s. Even at the highest temperature of 130°C, the maximum K value is 10x10⁻⁸/s for V835. Furthermore the viton material possesses the high deformation rate.

A more detailed analysis was conducted for the sample exposed to the inert gas environment. Figure C1 shows the temperature dependence of the relaxation rate constant K together with the error bar. The datum at 130°C for S383 is missing since this sample broke during exposure. It is evident that for the three materials examined, the relaxation rate increases with increasing temperature as expected. Since the degradation process should be thermally activated, activation energy can be obtained by using an Arrhenius analysis as shown in Figure C2 (log of the K_{th} versus 1/T). Activation energies of 1.46, 0.76 and 1.84 kcal/mole were obtained for V835, S650 and S383 respectively from the slope of the three lines in Figure C2. These energies are the controlling factor for the modification of the bond structure of the chain by thermal activation.

Table C1. Residual Strain After One Week in Inert Gas at Room Temperature

	2"	1.5"	1"	0.5"	Ave/Error	K ($10^{-8}/s$)
V835	0.017	0.017	0.016	0.016	0.017/0.001	5.72
S650	0.016	0.011	0.011	0.016	0.014/0.003	4.70
S383	0.009	0.015	0.018	0.012	0.014/0.005	4.70

Table C2. Residual Strain After One Week in an Inert Gas at 100°C

	2"	1.5"	1"	0.5"	Ave/Error	K ($10^{-8}/s$)
V835	Broken					
S650	0.020	0.025	0.019	0.016	0.020/0.005	6.75
S383	0.031	0.025	0.024	0.024	0.025/0.005	8.83

Table C3. Residual Strain After One Week in an Inert Gas at 130°C

	2"	1.5"	1"	0.5"	Ave/Error	K ($10^{-8}/s$)
V835	0.064	0.060	0.062	0.062	0.062/0.002	10
S650	0.038	0.037	0.038	0.038	0.038/0.001	6.53
S383	Broken					

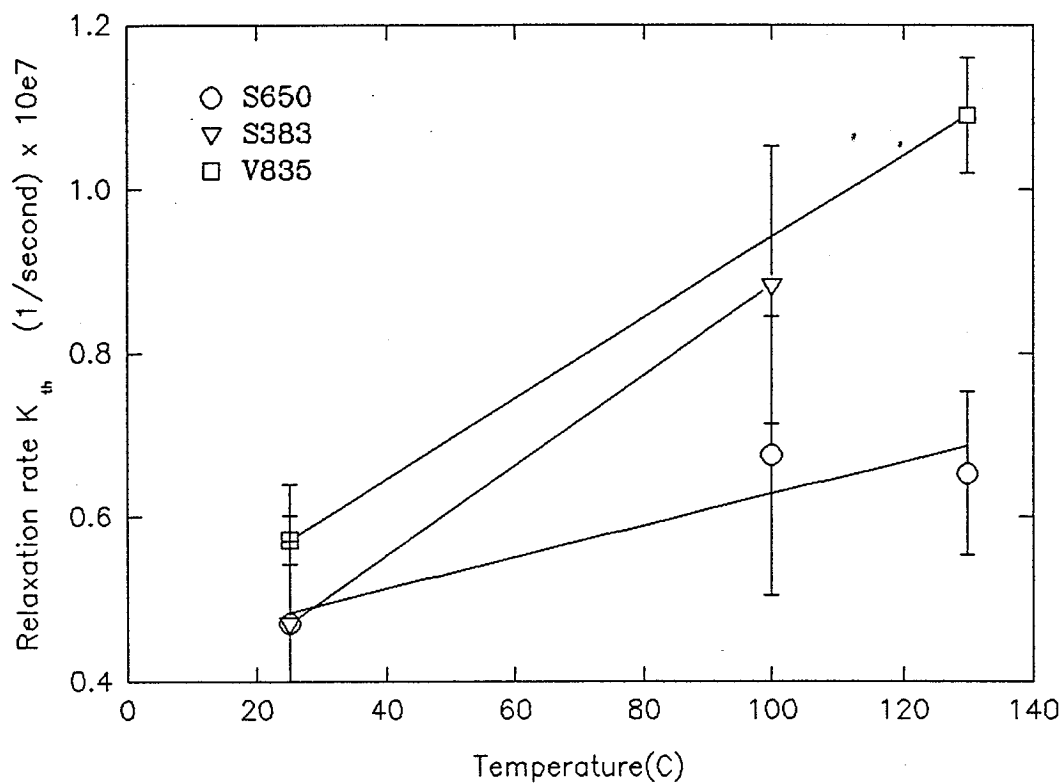


Figure C1. Relaxation rate for the three elastomers as a function of temperature when exposed to an inert gas environment (physical degradation only).

Thermal activation energy

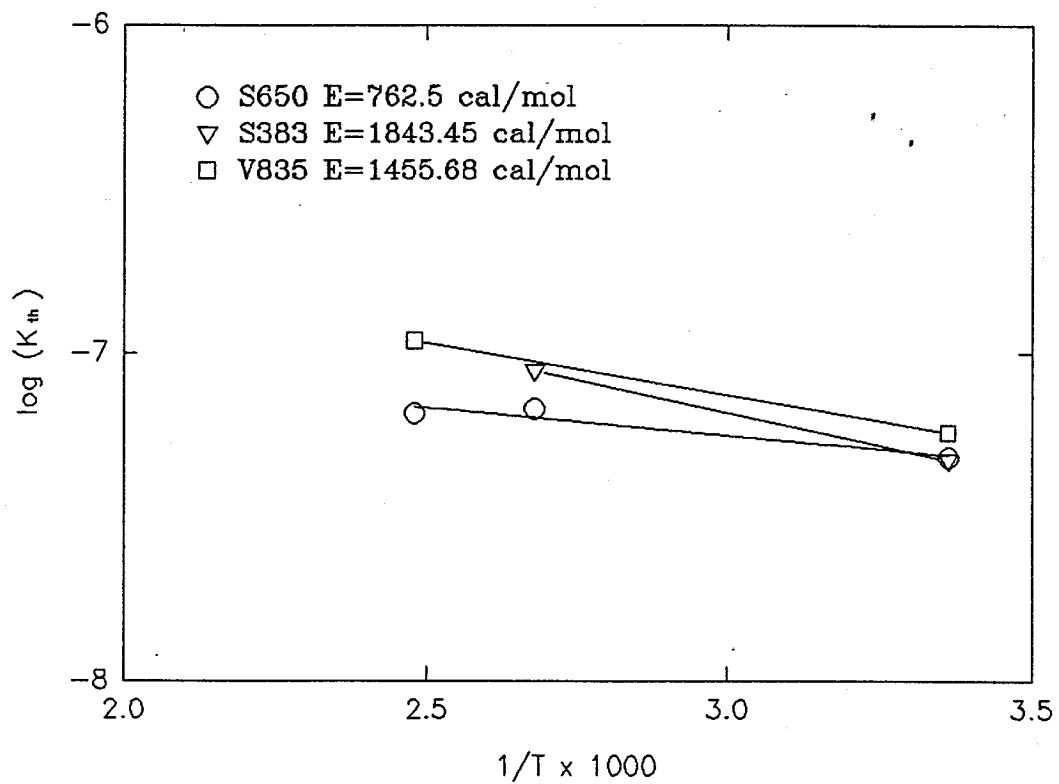


Figure C2. Arrhenius plot for the physical degradation process.

(D) Effects of Vacuum

The effects of vacuum on stress relaxation in three materials were examined using a special vacuum system at Auburn. A set of experiments to examine the effects of vacuum on stress relaxation in elastomeric materials were conducted. Stress relaxation tests were conducted in vacuum at 100°C. Heating was achieved by using resistive heating tapes. A set of reference tests were also performed at the same temperature but in air to isolate the effects of vacuum if any. Three materials were examined: S383, S650 and V835. The elastomers were put in a tension rig with a strain of 50%. A single experiment was conducted in vacuum at 100°C for one week. A diffusion pump station was used for this experiment providing a vacuum of 10^{-6} torr. Results from this test were given in Table D1. Similar to the observation in the inert tests, the viton material (V835) possesses the highest relaxation rate. Unfortunately, the V835 sample tested in inert gas failed prematurely at 100°C. Nonetheless, the K value for this material crept in vacuum at 100°C is higher than the relaxation rate in inert gas at a higher temperature of 130°C, indicative of the vacuum outgassing effect. The silicone base materials appear to be less susceptible to outgassing.

Table D1. Residual Strain After One Week in Vacuum at 100°C

	2"	1.5"	1"	0.5"	Ave/Error	K ($10^{-8}/s$)
V835	0.057	0.053	0.052	0.052	0.054/0.003	18.9
S650	0.025	0.021	0.023	0.018	0.022/0.004	7.55
S383	0.016	0.011	0.010	0.014	0.013/0.003	4.35

(E) Relaxation in Air

Three tests were conducted on V835, S650 and S383 (all at 50% strain) at 60°C, 100°C and 130°C. The durations selected were one week and two weeks. Unfortunately the S383 sample at 130°C broke and no relaxation datum was available. Tables E1 to E3 summarize the test results.

The relaxation rates of all three materials at all three temperatures are higher than the inert atmosphere standard (see Tables C1 to C3). This increase in the deformation rate could arise from any of the gaseous phases in air. However, a more detailed analysis using pure oxygen, to be discussed in the next section, will clearly illustrate that this is due to the presence of oxygen in air.

Table E1. Residual Strain After One Week in Air at 60°C

	2"	1.5"	1"	0.5"	Ave/Error	K (10 ⁻⁸ /s)
V835	0.047	0.047	0.047	0.044	0.046/0.002	16.0
S650	0.022	0.019	0.017	0.016	0.019/0.003	6.4
S383	0.018	0.019	0.017	0.014	0.017/0.003	5.27

Table E2. Residual Strain After One Week in Air at 100°C

	2"	1.5"	1"	0.5"	Ave/Error	K (10 ⁻⁸ /s)
V835	0.065	0.064	0.066	0.057	0.063/0.006	22.3
S650	0.021	0.017	0.013	0.020	0.018/0.005	6.07
S383	0.029	0.027	0.026	0.022	0.026/0.004	8.83

Table E3. Residual Strain After Two Week in Air at 130°C

	2"	1.5"	1"	0.5"	Ave/Error	K ($10^{-8}/s$)
V835	0.104	0.102	0.101	0.106	0.103/0.003	19.1
S650	0.064	0.065	0.063	0.060	0.063/0.003	11.1
S383	Broken					

(F) Effects of Oxygen

To clearly identify the role of oxygen in the relaxation process, a series of experiments were conducted with the materials exposed in pure oxygen at 100°C and 130°C. The data from these tests are given in Tables F1 and F2 below. These results are illustrated in a graphical manner in Figure F1. It is important to note that the presence of oxygen has significantly enhanced the relaxation rate in all three materials examined (K values are all on the order of $10^{-7}/s$). This oxygen effect can be seen in Figure F2 where the relaxation rates of the materials are plotted as a function of oxygen content in the environment. The zero oxygen data were taken from the inert gas experiments whereas the 21% oxygen conditions correspond to the air

environment. It is evident that there exist a near linear relationship between relaxation and oxygen. This is most likely a consequence of the chain breaking effect that occurs.

Table F1. Residual Strain After One Week in Pure Oxygen at 100°C

	2"	1.5"	1"	0.5"	Ave/Error	K (10 ⁻⁸ /s)
V835	0.091	0.089	0.090	0.088	0.090/0.002	32.7
S650	0.046	0.045	0.045	0.044	0.045/0.001	15.5
S383	0.057	0.057	0.057	0.060	0.058/0.002	20.3

Table F2. Residual Strain After One Week in Pure Oxygen at 130°C

	2"	1.5"	1"	0.5"	Ave/Error	K (10 ⁻⁸ /s)
V835	0.090	0.100	0.101	0.094	0.096/0.006	35.3
S650	0.095	0.103	0.103	0.100	0.102/0.007	37.7
S383	0.108	0.118	0.121	0.112	0.116/0.008	43.7

Change of K in pure oxygen with temperature

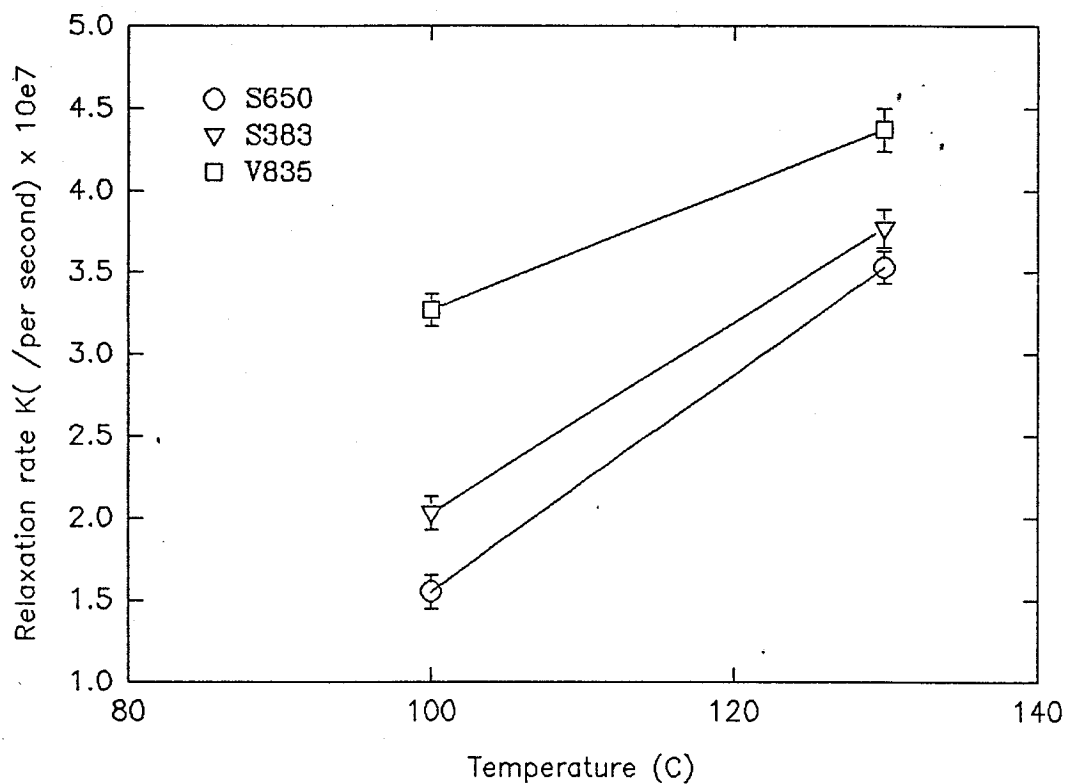


Figure F1. Relaxation rate as a function of temperature for the elastomers exposed to a pure oxygen environment.

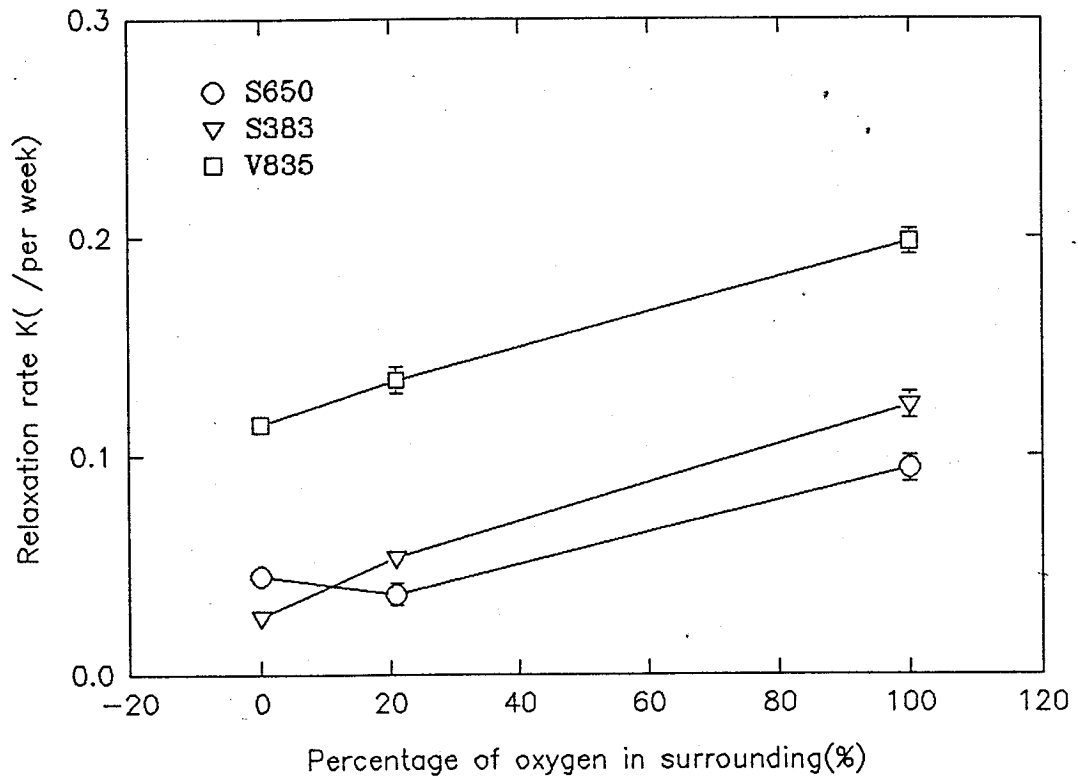


Figure F2. Effect of oxygen content on relaxation rate.

(G) Effects of Gamma Irradiation

The effects of gamma irradiation were examined using the high intensity Cobalt-60 source at Auburn University. In this portion of the study, a fourth material was introduced (V747) for the room temperature test. This source produced 1.3 MeV gamma ray. A special sample holder was designed and constructed to facilitate irradiation of the strained samples at elevated temperature in a vacuum. Heating was accomplished by surrounding the stainless steel sample holder tube with heater tape. Experiments were conducted at ambient temperature and at 100°C for a duration of one week. Results are summarized in Tables G1 and G2. It is evident that the presence of gamma significantly enhances the relaxation rate in the four materials. The K values are all in the $10^{-6}/s$ range, a two orders of magnitude increase from the $10^{-8}/s$ range for the pure thermal degradation effect. Figure G1 shows the temperature dependence of the relaxation rate. In this figure the thermal component of the relaxation rate (from Tables C1 to C3) has been subtracted out. It is evident that the pure irradiation effect on relaxation is extensive. Furthermore this effect increases with increasing temperature clearly illustrating the synergistic effect of the thermal and the irradiation-induced degradation processes. A preliminary experiment was also conducted where the samples were exposed to gamma but in the relaxed state. These samples were subsequently tested without irradiation. Limited data from this study show that the presence of gamma alone do not affect the relaxation property indicating that the chain breaking process due to irradiation only occurs in the simultaneous

presence of stress during irradiation.

Two samples, V835 and S383, were also irradiated in the relaxed state (not stretched) at room temperature for one day and seven days respectively in the gamma facility. Dynamic mechanical thermal analysis (DMTA) was conducted on the unirradiated standards and the irradiated materials. Figures G2 and G3 show the $\tan \delta$ (loss tangent) dependence on temperature for the unirradiated materials and Figures G4 to G5 show the same parameter for the irradiated elastomers. No significant changes were detected. The T_g of the materials remains at about -15°C and -102°C for viton and silicone rubber respectively. This appears to be in contradiction with the stress relaxation experiments which exhibited large relaxation due to gamma irradiation (even at room temperature). This is due to the unstress condition of the specimens tested with DMTA and clearly indicates the importance of stress on the observed effects of gamma. The chain modification process by radiation in the absence of stress is significantly less pronounced than that in the presence of stress due to synergistic effects of the two.

Table G1. Residual Strain After One Week in Gamma at Room Temperature

	2"	1.5"	1"	0.5"	Ave/Error	K ($10^{-8}/s$)
V835	0.327	0.318	0.312	0.314	0.317/0.010	166
S650	0.325	0.318	0.317	0.314	0.318/0.007	167
S383	0.341	0.342	0.341	0.346	0.343/0.003	192
V747	0.313	0.313	0.313	0.306	0.312/0.006	162

Table G2. Residual Strain After One Week in Gamma at 100°C

	2"	1.5"	1"	0.5"	Ave/Error	K ($10^{-8}/s$)
V835	0.360	0.355	0.351	0.353	0.355/0.005	205
S650	0.402	0.400	0.396	0.393	0.398/0.005	263
S383	0.379	0.378	0.374	0.376	0.377/0.003	232

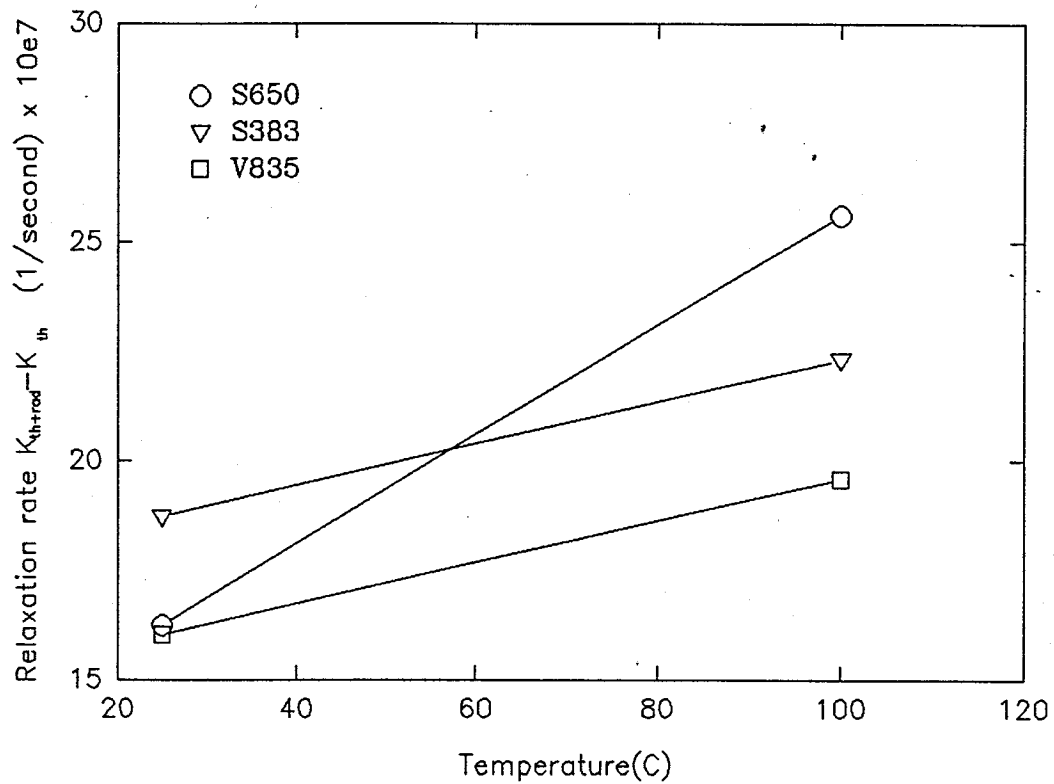


Figure G1. Relaxation rate of the elastomers as a function of temperature due to gamma irradiation.

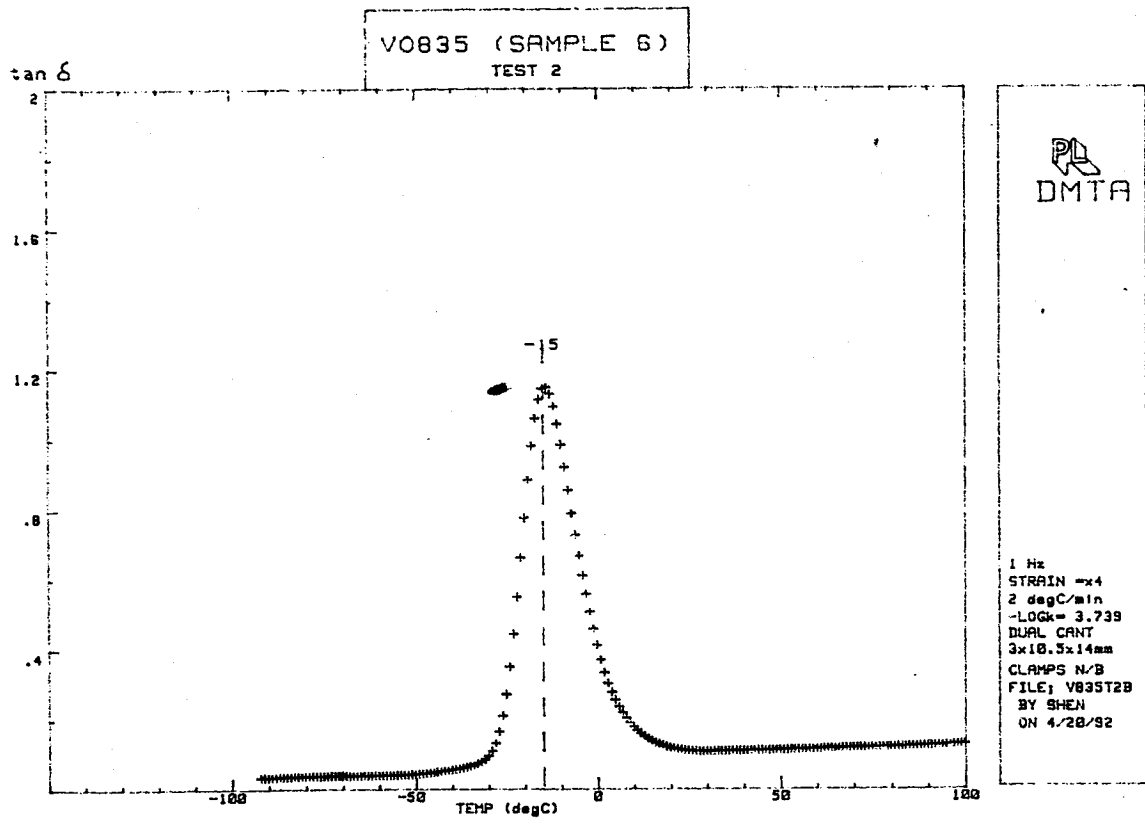


Figure G2. Loss tangent (tan δ) of V835 as a function of temperature prior to irradiation.

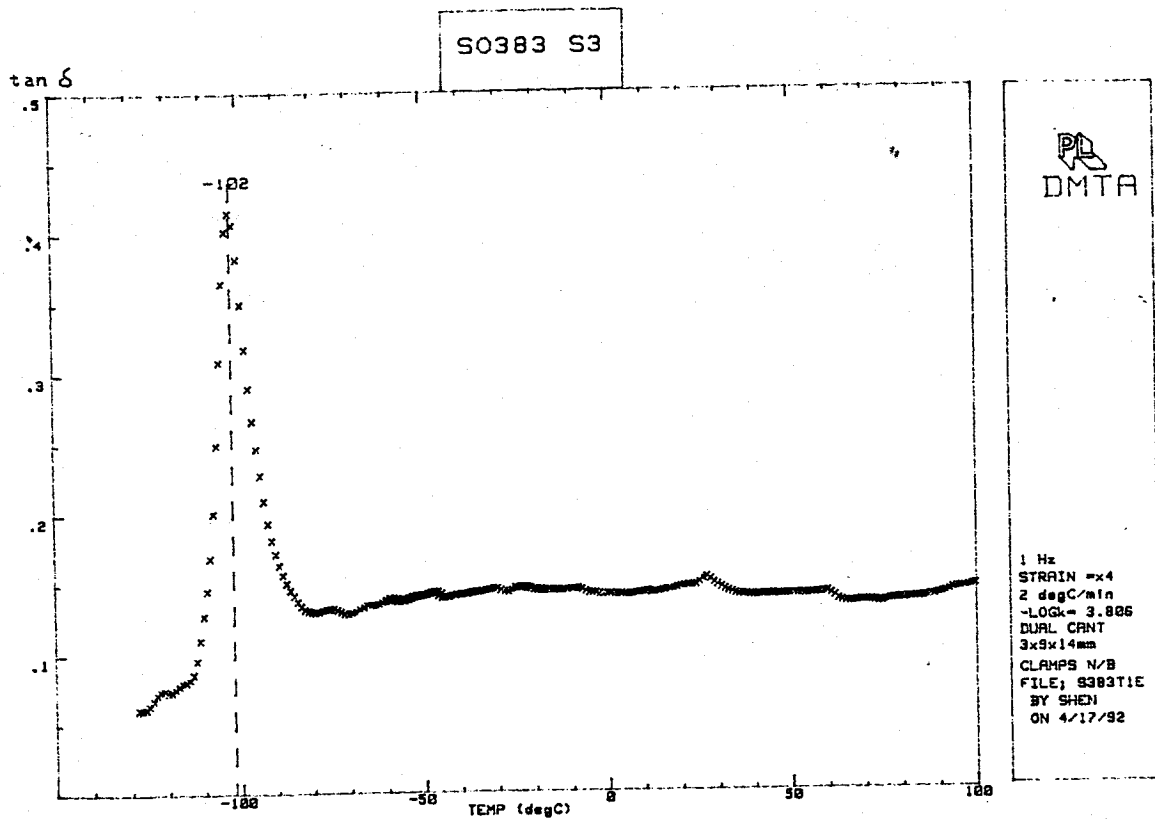


Figure G3. Loss tangent ($\tan \delta$) of S383 as a function of temperature prior to irradiation.

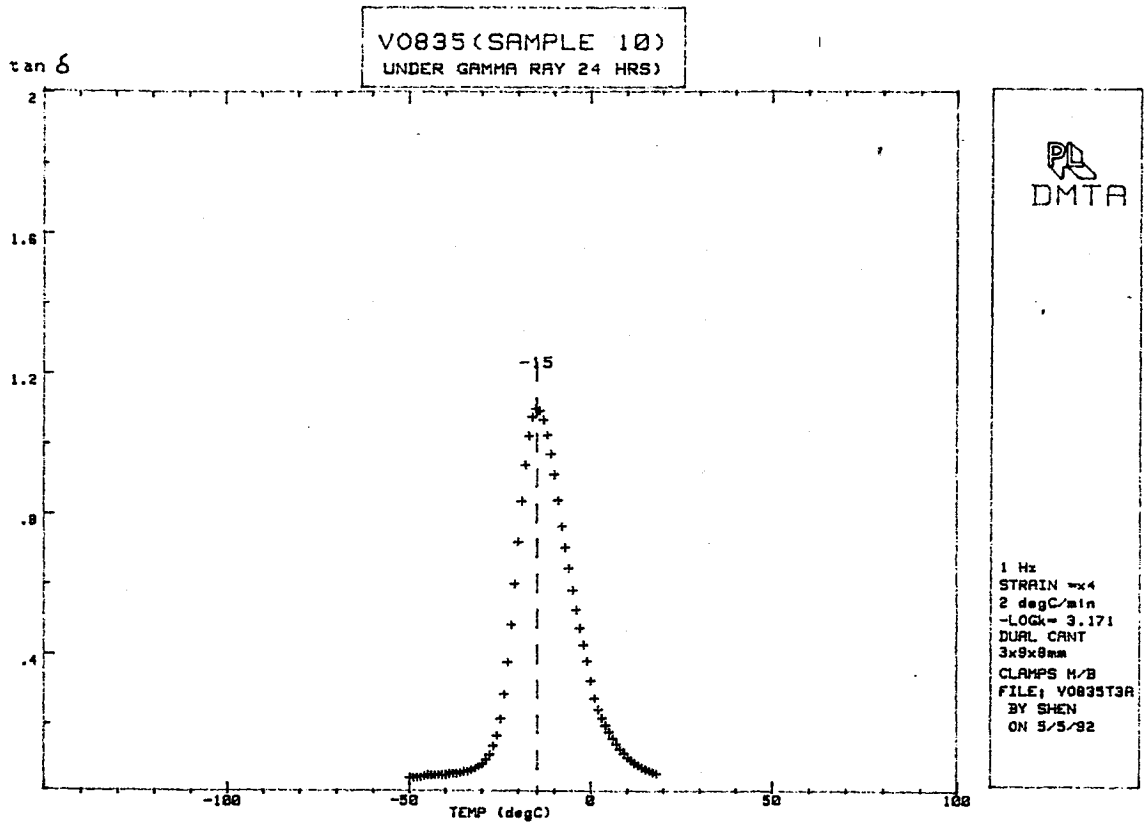


Figure G4. Loss tangent ($\tan \delta$) of V835 as a function of temperature after irradiation.

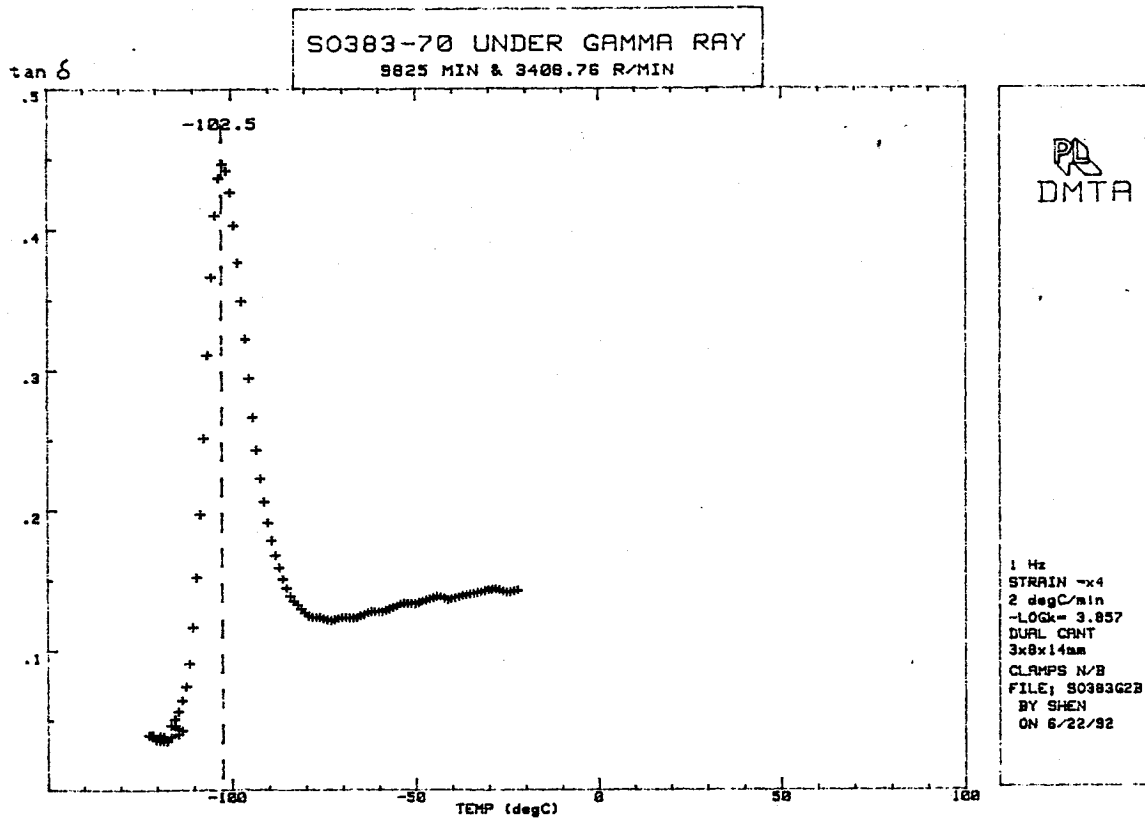


Figure G5. Loss tangent ($\tan \delta$) of S383 as a function of temperature after irradiation.

(H) Effects of Proton Irradiation

A set of S383 specimens were irradiated with 2 MeV protons at MSFC to doses up to 1.4×10^{15} protons/cm² at room temperature. A series of DMTA tests were conducted on the pre-irradiated and irradiated specimens at different frequencies as a function of temperature. The E' , E'' and $\tan \delta$ variations with temperature and test frequencies for the unirradiated S383 are shown in Figures H1 to H3. Similar results for the irradiation material are given in Figures H4 to H6. The shift in the maxima in the $\tan \delta$ versus temperature plot (corresponding to T_g) at different excitation frequencies is related to the activation energy of the deformation process. This phenomenon is illustrated in Figure H7 where the slope of the curve corresponds to the activation energy. Values of 38 and 54 kcal/mole were obtained for the S383 material in the unirradiated and irradiated conditions respectively.

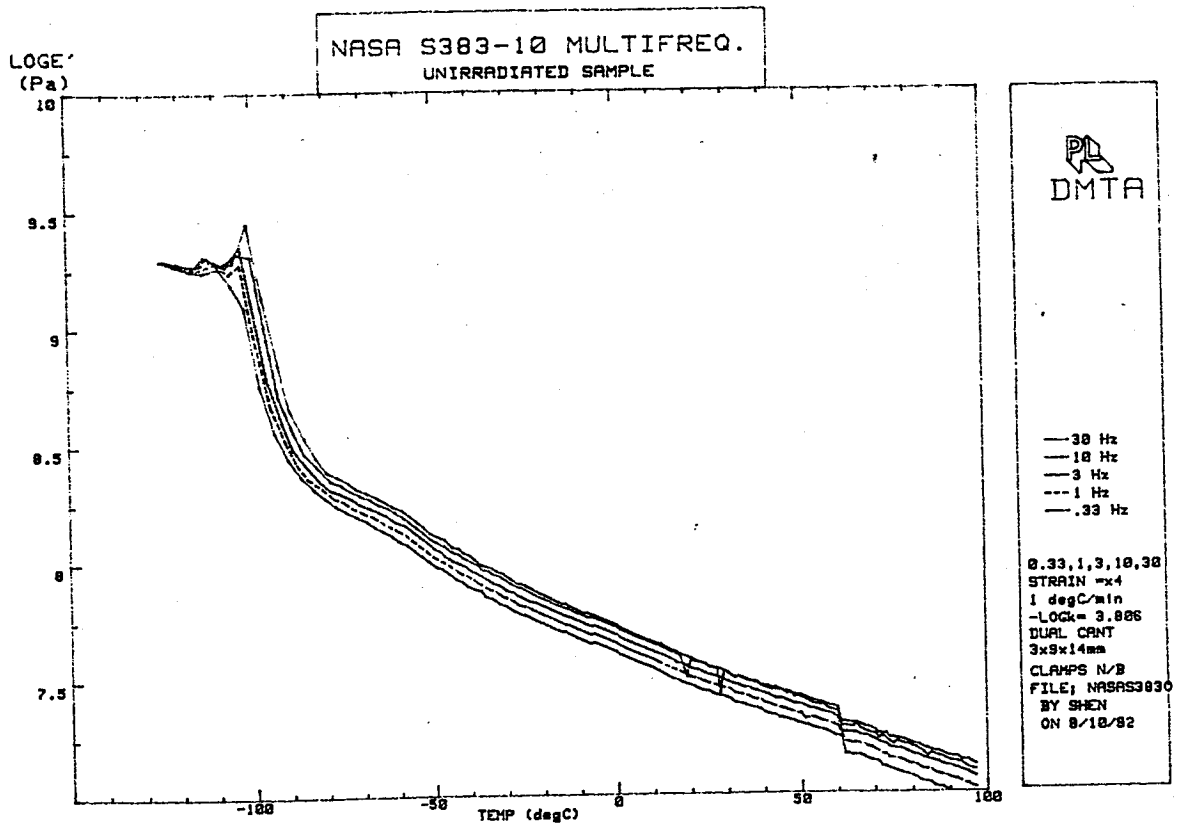


Figure H1. Variation of E' as a function of temperature for different excitation frequencies for S383 prior to proton irradiation.

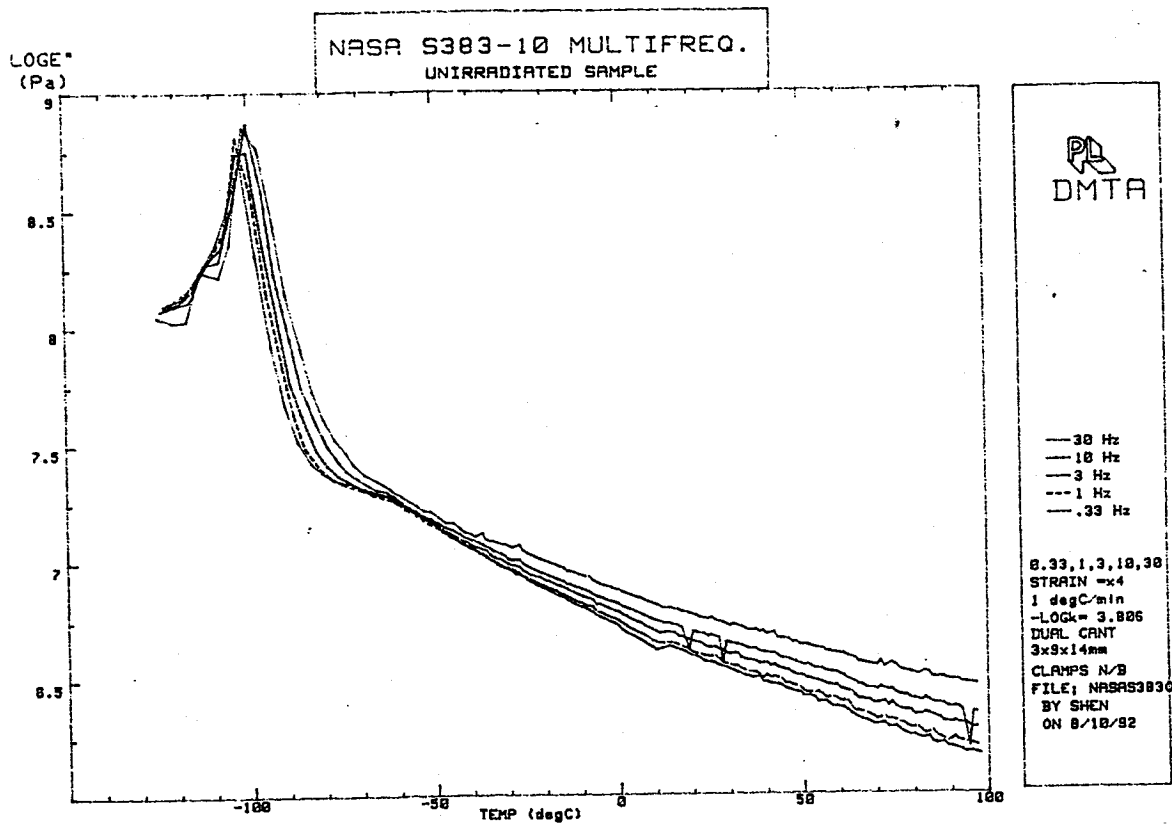


Figure H2. Variation of E'' as a function of temperature for different excitation frequencies for S383 prior to proton irradiation.

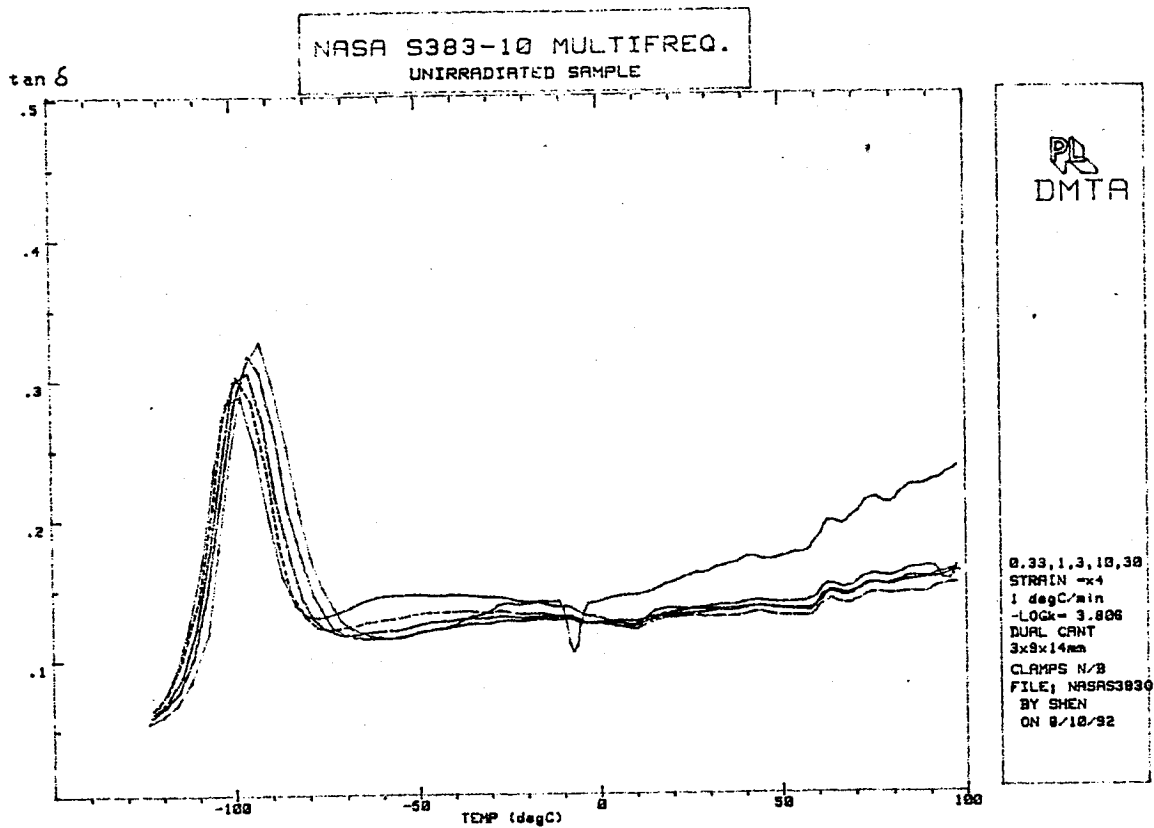


Figure H3. Variation of $\tan \delta$ as a function of temperature for different excitation frequencies for S383 prior to proton irradiation.

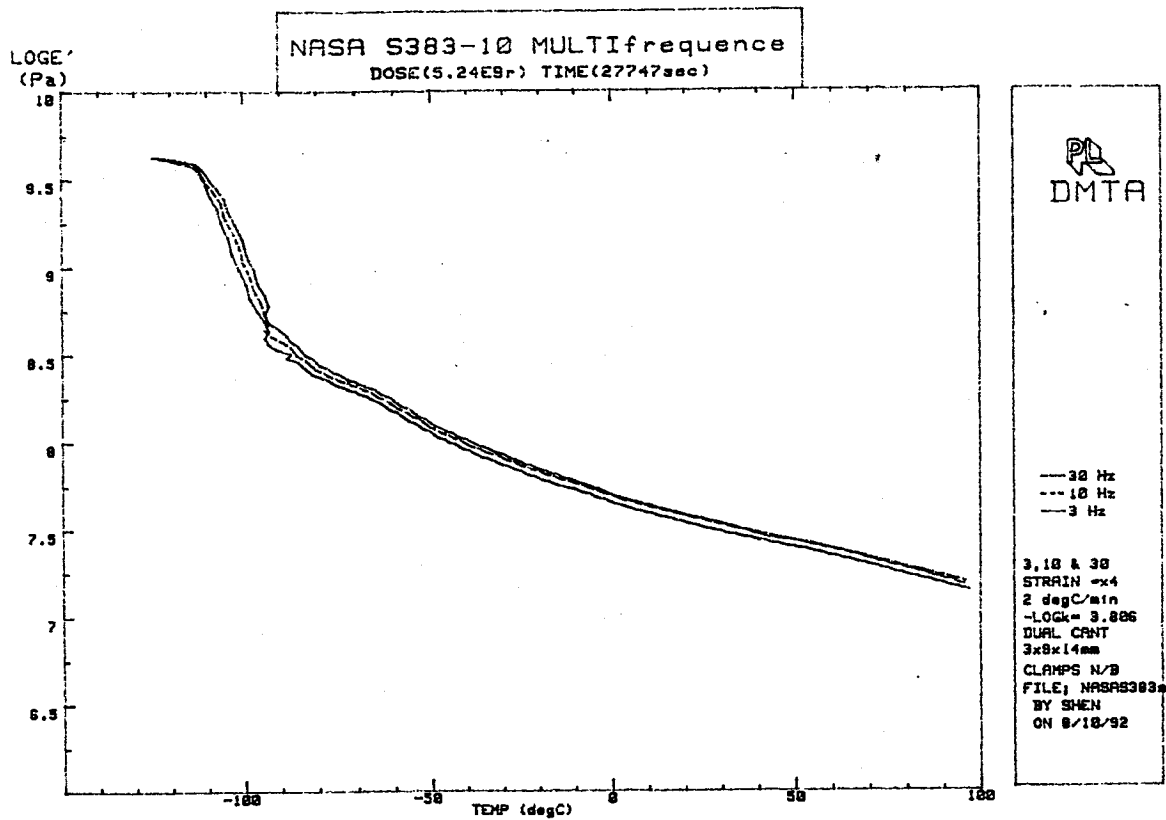


Figure H4. Variation of E' as a function of temperature for different excitation frequencies for S383 after proton irradiation.

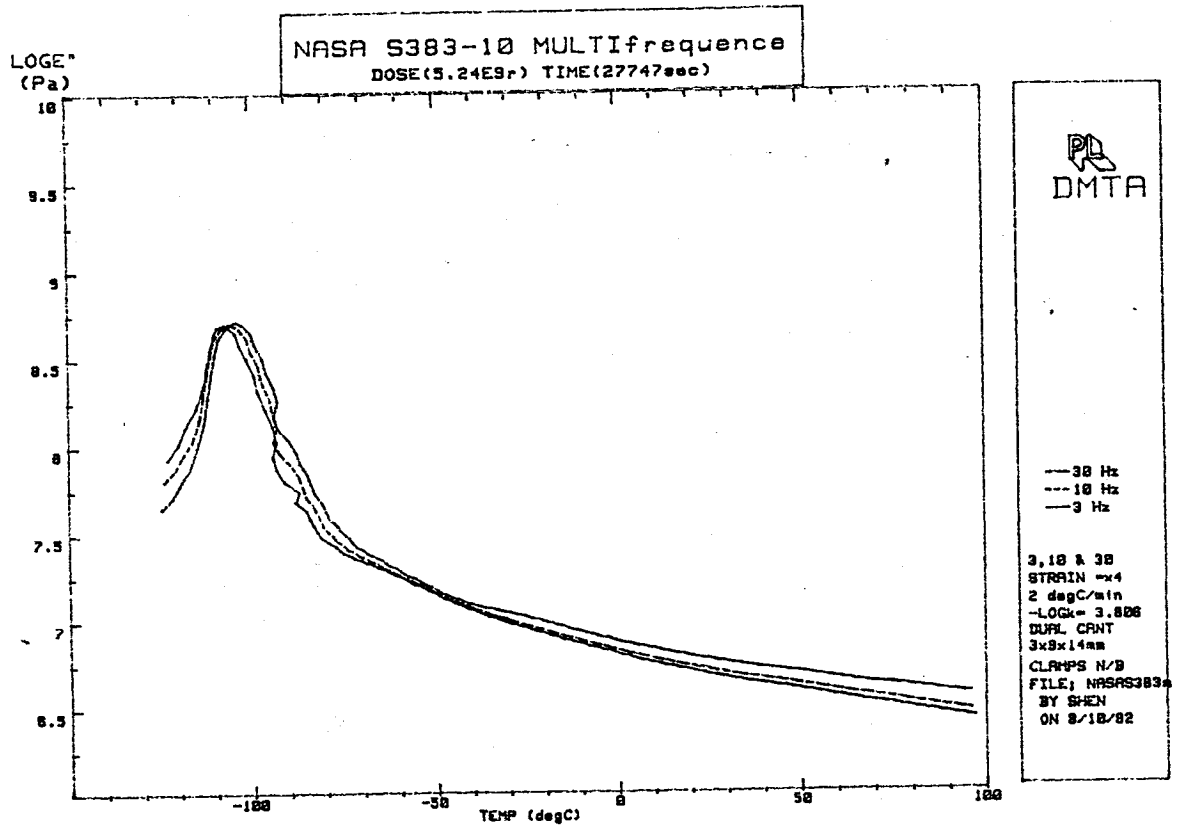


Figure H5. Variation of E'' as a function of temperature for different excitation frequencies for S383 after proton irradiation.

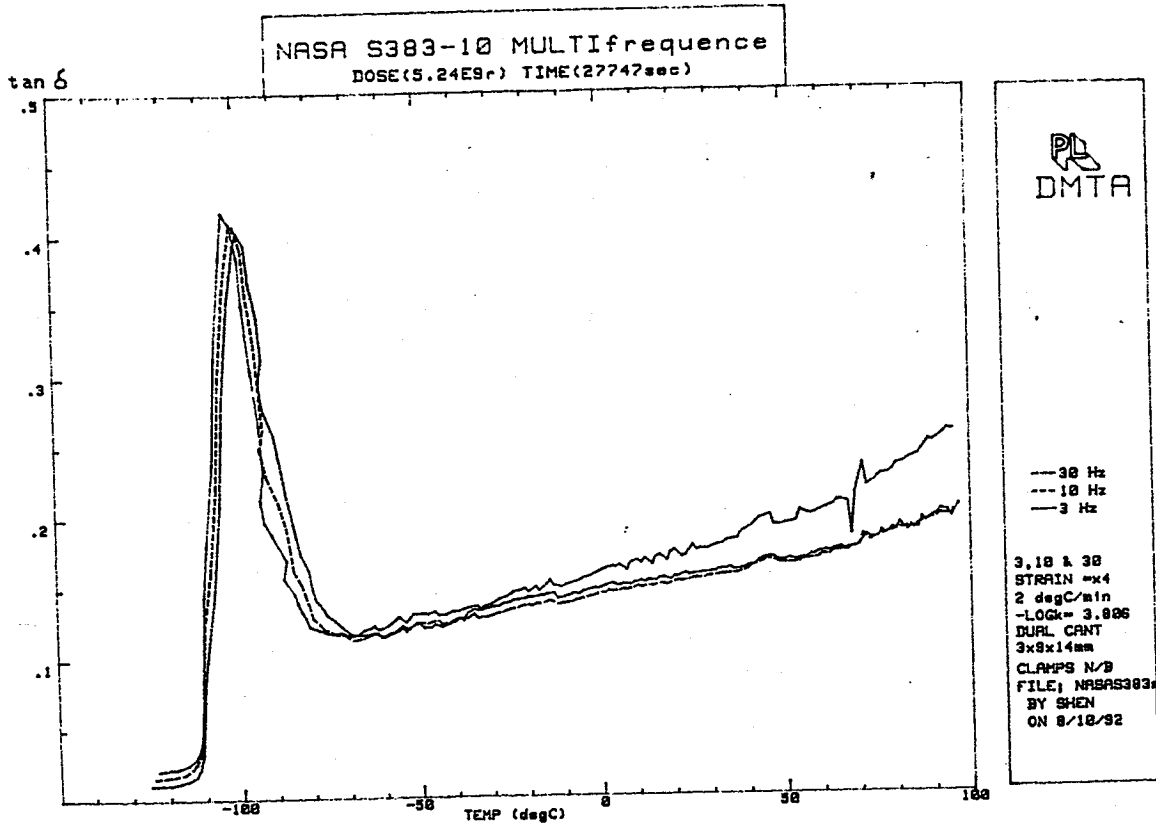


Figure H6. Variation of $\tan \delta$ as a function of temperature for different excitation frequencies for S383 after proton irradiation.

NASA S383-10

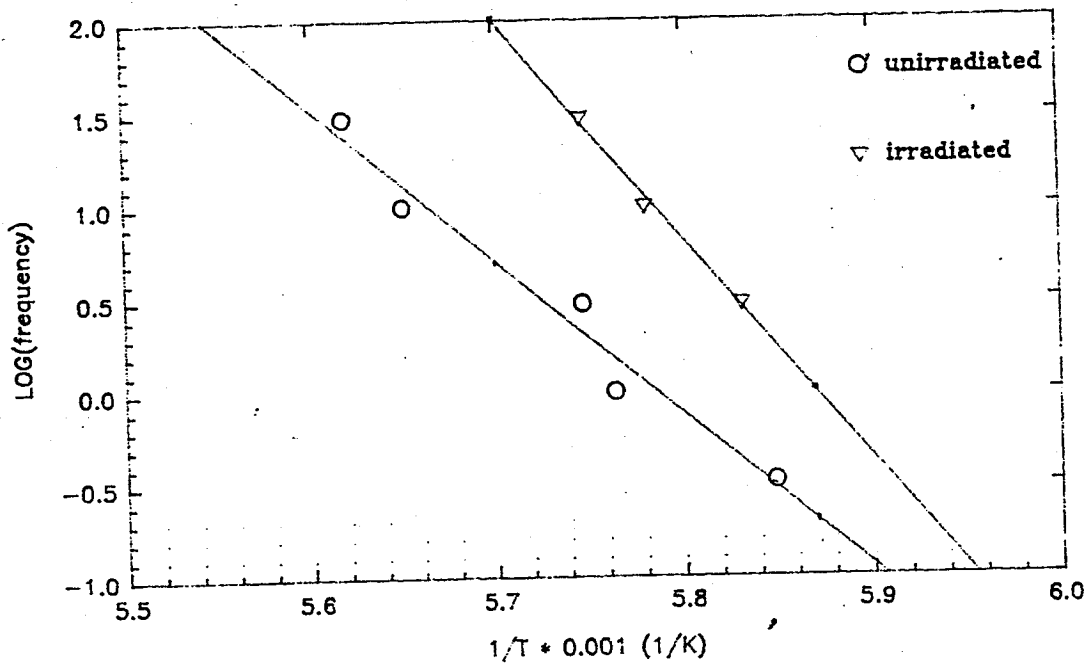


Figure H7. Arrhenius plot illustrating the effect of proton irradiation on activation energy.

V. Conclusions

The relaxation behavior of different elastomeric materials (V835, S383 and S650) was examined using available information and new data generated by this project. Tests were conducted (in a pseudo stress relaxation mode) to examine the effect of thermal outgassing (or thermal vacuum), oxygen, inert gas, gamma radiation and proton irradiation on the degradation process from ambient temperature to 130°C. As a result of this one year program, the following observations were made:

- (1) Data available in the literature were successfully fitted to a universal curve for lifetime prediction from which activation energies were obtained and a refined physical model was established. Activation energies for deformation were determined to be 12, 18, 9 and 8.5 kcal/mole for V835, S383, S650 and V747.
- (2) The viton material (V835) possessed higher relaxation rates than the silicone materials and it also exhibited limited outgassing effect.
- (3) The main effect of air in all three materials was determined to be from oxygen. The presence of oxygen enhanced the relaxation rate in a proportional manner.
- (4) The simultaneous application of gamma radiation and stress was found to dramatically increase the relaxation rate (by two orders of magnitude). The elastic properties of the elastomers were not affected by the sole presence of gamma.
- (5) Proton irradiation, in the absence of simultaneous application of stress, did not have a significant effect on the elastic property of the elastomers.

VI. References

1. D.E. Morris, "Estimation of Life of Seal Materials for Space Station Freedom," Test Report # EH33/91-2, NASA Marshall Space Flight Center (1991).
2. I.M. Ward, "Mech. Properties of Solid Polymers," 2nd Ed. Wiley Sci. Pub. New York (1983).
3. U. Eisele, "Introduction to Polymer Physics," Springer-Verlag, Berlin and New York (1990).
4. F. Schwarzl and A.J. Savermann, *Physics* 18 (1952) 791 and *Appl. Sci. Res.* A4 (1953) 127.
5. J.D. Ferry and M.L. Williams, *J. Colloid Sci.*, 7 (1953) 347 and *J. Polymer Sci.*, 11 (1953) 169.
6. M. Ito, S. Okada and I. Kiriya, *Rep. Prog. Polym. Phys. Jap.*, 21 (1978) 247.
7. M. Ito, S. Okada and I. Kiriya, *Rep. Prog. Polym. Phys. Jap.*, 22 (1979) 541.
8. M. Ito, S. Okada and I. Kiriya, *Radiat. Phys. Chem.*, 16 (1980) 481.
9. M. Ito, *Radiat. Phys. Chem.*, 17 (1981) 203.
10. M. Ito, *Polymer*, 23 (1982) 1515.
11. M. Ito, *Radiat. Phys. Chem.*, 21 (1983) 459.
12. M. Ito, *Radiat. Phys. Chem.*, 31 (1988) 615.

CN22 (0) (2)
TURNER J/PUBLICATION
MARSHALL SPACE FLIGHT CENTER
HUNTSVILLE AL.

DELETIONS OR CHANGES 544-4494
RETURN ADDRESS CN22D 000002444